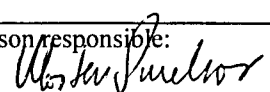


Report 2001.060

**Interpretation of potential field
data from the Nordland VI-VII area**

Report no.: 2001.060	ISSN 0800-3416	Grading: Åpen	
Title: Interpretation of potential field data from the Nordland VI-VII area			
Authors: Odleiv Olesen		Clients: Norsk Hydro and Enterprise Oil Norge	
County: Nordland and Troms		Commune:	
Map-sheet name (M=1:250.000) Bodø, Svolvær, Narvik, Andøya and Tromsø		Number of pages: 51	Price (NOK): 290
Fieldwork carried out:		Date of report: 23.10.2001	Project no.: 2905.00
		Person responsible: 	
<p>Summary:</p> <p>Aeromagnetic and gravity data from the Lofoten area have been compiled, processed and interpreted. Forward 2.5D modelling along two profiles is constrained by available data on density, magnetic properties and reflection and refraction (OBS) seismics. A basement structure map including depth to magnetic basement, regional basement faults and transfer zones is compiled. Several rifting events from the Permian to Tertiary have resulted in a shallow Moho, uplifted core complexes and rotated basement-blocks separated by transfer zones. The Bivrost, Mosken, Melbu, Vesterålen and Lenvik transfer zones are located where shifts in polarity occur along the faults and separate individual rotated fault blocks. The depth to basement is c. 5 km in the Ribban Basin offshore Lofoten and 9 km in the Røst Basin. Greater depths to magnetic basement occur locally. We interpret these most likely to represent down-faulted Caledonian nappes, Devonian sediments or low-magnetic (amphibolite facies) Precambrian rocks. Voluminous mafic intrusions occur in both the basement and the overlying sediments in the Sandflesa area and cause large gravity and magnetic anomalies. This volcanic complex may represent a precursor (sea-mount) to the final opening of the Atlantic Ocean. Rotated fault blocks situated between the Røst Basin and Utrøst Ridge immediately to the northeast of the Sandflesa area most likely also contain mafic intrusions. The depth extent and age of these intrusive rocks can, however, not be resolved from the potential field data. A late Cretaceous-Early Tertiary age is likely because the area is located adjacent to the Vøring volcanic province. This scenario has implication on the maturation of source rocks and consequently the petroleum potential in the western Nordland VI-area. Basement depth estimates from both gravity and magnetic data to the north of the Marmæle Spur show that there may be an approximately 2 km thick sequence of low-density sediments below the base-Cretaceous in this area. The quality of the multichannel seismics is poor in this particular area due to the pronounced sea floor multiples.</p> <p>The high-frequency anomaly pattern evident in the compilation of modern high-resolution surveys is interpreted to have three different types of magnetic sources; a) Quaternary overburden of varying thickness and bathymetric features, b) sub-cropping sedimentary units, c) Flow basalts and sills, notably along the western margin of the Utgard High and Utrøst Ridge up to Andøya.</p> <p>I suggest that both the 200 km wide negative gravity anomaly in the Vestfjorden-Sarek area and the Neogene uplift of the region may be caused by low-density material mantle emplaced by small-scale convection or diapirism within the asthenosphere. The Lofoten-Vestfjorden-Sarek region may be in isostatic equilibrium due to the opposing effects of positive and negative gravity anomalies. This model explains the Plio-Pleistocene uplift and exhumation of the Lofoten-Vesterålen continental shelf.</p>			
Keywords: Geofysikk	Kontinentalsokkel	Tolkning	
Berggrunnsgeologi	Magnetometri	Forkastning	
Petrofysikk	Gravimetri	Fagrapport	

CONTENTS

1 INTRODUCTION.....	4
2 DATA SETS.....	4
2.1 Aeromagnetic data	4
2.2 Gravity data	6
2.3 Petrophysical data	7
2.4 Bathymetric and topographic data.....	10
3 INTERPRETATION METHODS	11
3.1 Interpretation of depth to anomaly sources	11
3.2 Image enhancements.....	12
3.3 GM-SYS interactive modelling.....	12
3.4 Geophysical interpretation map.....	13
4 STRUCTURAL FRAMEWORK.....	14
5 RESULTS.....	15
5.1 Regional basement configuration - transfer zones.	15
5.2 Sandflesa area.....	16
5.3 Lofoten - Vesterålen area.....	18
5.4 Neogene uplift.....	19
5.5 Internal basin structures	19
6 CONCLUSIONS.....	20
7 RECOMMENDATIONS FOR FURTHER WORK.....	22
8 ACKNOWLEDGEMENTS.....	22
9 REFERENCES.....	23
List of figures and tables	28

1 INTRODUCTION

The present study of potential field data is carried out as part of the Nordland VI-VII project financed by the Enterprise Oil Norge - Norsk Hydro AMI. The survey area extends from 66°45' to 69°45'N and from the oceanic crust to the west (spreading anomaly 22) eastward to the Swedish border. The focus area shifted towards the Sandflesa area during the interpretation work (Figs. 1 & 2). The database includes existing aeromagnetic and gravity surveys (Figs. 3 & 4) in the area: NGU-73 (northern Vøring Basin), LAS-89 (Lofoten Aeromagnetic Survey 1989), northern part of the NAS-94 Survey (Nordland Aeromagnetic Survey 1994), VAS-98 (Vestfjorden Aeromagnetic Survey 1998), HRAMS-97/98 (Andfjorden and Harstad Basin) and an offshore gravity compilation provided by Norsk Hydro. Additional gravity and aeromagnetic data from the adjacent areas have been included to ease the interpretation of the regional structures.

2 DATA SETS

2.1 Aeromagnetic data

A total of eight offshore aeromagnetic surveys (Fig. 3) have been compiled and interpreted in the present project. Specifications for these surveys are shown in Table 1. Vintage data that were re flown in 1989, 1994 and 1998 are not included in the table, and are also excluded in the final map compilation. The pattern of flight lines generally provides data along NW-SE trending lines with a spacing of 2-5 km. The LAS-89 and NGU-73 surveys have been reprocessed using the differential median technique (Mauring *et al.* in press).

Aeromagnetic data on land have earlier been digitised into a 500 x 500 m matrix and the Definite Geomagnetic Reference Field (DGRF) has been subtracted (Nor. geol. unders. 1992). The area was flown at different flight altitudes and line spacing dependent on the topography. Specifications for the different sub-areas are given in Table 2. The grids were trimmed to c. 10 km overlap and merged using a minimum curvature algorithm, GRIDKNIT, developed by Geosoft (2000a). The final grid shown in Figs. 5 & 6 was displayed using the shaded-relief technique with illumination from the southeast. To enhance the high frequency component of the modern LAS-89, NAS-94, Vestfjorden-98 and HRAMS-97/98 surveys, an 8 km Gaussian high pass filtered map of the compiled data-set has been produced (Fig. 6). The location of flow basalts and sills and sediment-related magnetic anomalies are more visible on this map than on the total field map. A grey tone shaded relief version of the high pass filtered grid is superimposed on the coloured total field map (Fig. 5).

Table 1. Offshore aeromagnetic surveys compiled for the present study (Figs. 3, 5 & 6).

Year	Area	Operator	Navigation	Sensor elevation m	Line spacing km	Recording	Length km
1969	69° - 70°N	NGU	Decca	200	4	Digital	1.000
1973	Vøring Basin	NGU	Loran C	500	5	"	6.000
1973	Norwegian Sea	NRL		300	10	"	1.000
1989	Lofoten	NGU	GPS/Loran C/Syledis	250	2	"	24.000
1994	Nordland Ridge	NGU	GPS	150	2	"	3.000
1998	Andfjorden	NGU	GPS	150	1	"	7.000
1998	Vestfjorden	NGU	GPS	150	2	"	6.000

Table 2. On land aeromagnetic surveys compiled for the present interpretation (Figs. 3, 5 & 6).

Year	Area	Operator	Navigation	Sensor elevation	Line spacing km	Recording
1964	Andøya	NGU	Visual	150 m above ground	1	Analogue
1965	Vesterålen area	NGU	Visual	300 m above ground	2	"
1971-73	Nordland-Troms	NGU	Decca	1000 m above sea level	2	"
1982	Norrbotten	SGU	Inertial	1800 m above sea level	2	Digital

2.2 Gravity data

The present study is based on measurements from 4600 gravity stations on land (Table 3 & Fig. 4) and approximately 20.000 km of marine gravity profiles collected by the Norwegian Petroleum Directorate, oil companies and the Norwegian Mapping Authorities in addition to gravity data from satellite altimetry in the deep-water areas of the Norwegian Sea (Andersen & Knudsen 1998). The complete Bouguer reduction (Mathisen 1976) of the gravity data has been computed using a rock density of 2670 kg/m³ on land. The simple Bouguer correction at sea was carried out using a density of 2200 kg/m³. The International Standardization Net 1971 (I.G.S.N. 71) and the Gravity Formula 1980 for normal gravity have been used to level the surveys. The compiled data-set has been interpolated to a square grid of 2 km x 2 km using the minimum curvature method. The isostatically corrected Bouguer anomaly map (Fig. 7) has been produced from this grid using the Oasis Montaj software system (Geosoft 2001). The procedure for the isostatic correction is described in section 3.1 below. A 100 km Gaussian high pass filtered map of the compiled data-set has also been produced (Fig. 8). These gravity data have been loaded into a Charisma workstation at the premises of Norsk Hydro in Harstad. The contour interval of the gravity maps in Figs. 7 & 8 are 5 and 2 mGal, respectively.

Table 3. Gravity surveys on land compiled in the present study (Fig. 4). The continental shelf area is covered by c. 20.000 km of marine gravity profiles. To produce the gravity maps in Figs. 7 & 8 additional data (2.5x2.5 km grid) from the adjacent part of northern Sweden (Henkel 1991) were included.

Survey stations	Area	No. of stations
Geological Survey of Norway	Nordland and Troms	3062
Norwegian Mapping Authority	Nordland and Troms	1183
Svela (1971)	Lofoten - Vesterålen	306
Saxov	Bardu	55
Total		4606

2.3 Petrophysical data

The pronounced magnetic and gravimetric anomalies within the project are continuous from land onto the continental shelf (Figs. 5 - 8). It is important to know the density and magnetic properties of the rocks on land when interpreting the potential field data in the offshore area. Approximately 2000 rock samples, collected during geological mapping and geophysical studies have been measured with respect to density, susceptibility and remanence (Olesen *et al.* 1997). An additional 2000 *in situ* susceptibility measurements were included from c. 200 localities in the Precambrian basement of Vesterålen and Senja (Mørk & Olesen 1995).

The high-amplitude magnetic anomalies in the Lofoten-Vesterålen and northwestern part of Senja are caused by granulite-facies gneisses and intrusives (mangerites). The Q-values are generally low, in the order of 0.5 or lower. Especially mafic and ultramafic rocks show, however, frequently high Q-values. These rocks give arithmetic means as high as 0.9 in the Lofoten area while the logarithmic mean is 0.3. Schlinger (1985) and Olesen *et al.* (1991) have also shown that the remanence of the rocks in the Lofoten-Vesterålen area is viscous and parallel to the present Earth's field, which make aeromagnetic interpretations in the area simpler.

The orthopyroxene isograd in the Vesterålen area coincides with the boundary between the high-magnetic and low-magnetic gneisses. The migmatites to the west of this line are in granulite-facies metamorphism whereas to the east they have amphibolitic metamorphic grade. In this particular area the magnetic basement surface reflects the depth to the granulite-facies gneisses. The medium amplitude magnetic anomalies on the mainland are mostly caused by granitic and quartz-dioritic rocks and migmatitic gneisses. The average density for all basement rocks in the Lofoten-Vesterålen area is 2780 kg/m³. The average density for the Middle Allochthon, which constitutes the bulk of the Caledonides within the Lofoten-Lopphavet area, is 2820 kg/m³.

As constraints for the gravity modelling I have used information from petroleum exploration wells to the south of the survey area. Density of sedimentary sequences calculated from well logs, refraction seismics and previous interpretation reports in the Nordland area is shown in Table 4. Numbers in parentheses show depth of base of the different sequences.

Table 4. Density (in 1000*kg/m³) of sedimentary sequences from density logs of wells in the Nordland area. (2.78*) = average density of 639 rock samples from the Precambrian on the Lofoten and Vesterålen archipelago (Olesen et al. 1997).

	Well 6609/7-1 Phillips Petroleum Nordland Ridge	Well 6607/5-1 Esso Utgard High	Well 6607/5-2 Esso Utgard High	Well 6507/2-1 Norsk Hydro Dønna Terrace	Norsk Hydro Int. Report (1998) Nordland VI area	Density estimates from refraction seismics Mjelde et al. (1998) Sandflesa area	Density adapted for modelling
Water depth	250m	368m		381m			1.03
Start of log	1025m	900m		1050m			
Pleistocene		2.21 (1220m)					
Plio-Pleistocene					2.03	2.00	2.03
Tertiary	2.10 (1635m)	2.21 (2510m)		2.18 (2005m)	2.12	2.15	2.23
Upper Cretaceous					2.23	2.20	
Lower Cretaceous					2.29	2.45	
Cretaceous	2.25 (1845m)	2.32 (3785m+)		2.37 (3610m)			2.35
Jurassic				2.54 (4400m+)	2.36	2.60	2.43
Triassic					2.51	2.60	2.43
Permian	2.31 (1920m)				2.51		
Eastern basement	2.64 (1960m+)				2.74	2.70	2.75 (2.78*)
Western basement						2.80	2.80-2.85
Lower crust						3.10-3.23	3.00-3.20
Sill			3792 m- 3886 m 2.92				2.95
Sill			4640 m- 4697 m 2.98				
Magmatic underplating							3.00-3.20
Mantle							3.30

Table 5. Seismic velocities (*1000 m/s) in the Nordland area.

Unit	Stacking velocity LO-06-86 Olesen & Torsvik (1993)	Stacking velocity TB-38-87 Olesen & Torsvik (1993)	Refraction seismics Sandflesa area Mjelde et al. (1998)	Refraction seismics Lofoten area Mjelde et al. (1993)	Refraction seismics Røst Basin Mjelde et al. (1992)	Norsk Hydro (1998) Nordland VI area	Velocity adapted for depth conversion of lines A-A' and B-B'
Sea water	1.48	1.48	1.48	1.48	1.48	1.48	1.48
Plio-Pleistocene			1.86	1.9	1.9	2.03	1.85
Tertiary sediments	3.1	2.3	2.67	3.1	2.4	2.30	2.30
Tertiary volcanics					4.8		
Upper Cretaceous			3.44	4.0		2.70	
Lower Cretaceous			4.64	5.1		3.00	
Cretaceous	3.2	4.5			4.5		2.90
Jurassic					4.5	3.40	
Triassic						4.30	
Jurassic-Triassic	4.5	6.0					3.90
Upper crustal basement				6.0	6.0		

Table 6. Magnetic properties of igneous rocks from drilling in the Vøring area within the Deep Sea Drilling Project (DSDP) and Ocean Drilling Program (ODP) in 1974 and 1985, respectively (¹Kent & Opdyke 1978, ²Eldholm et al. 1987). The ODP susceptibility data are claimed to be cgs-units, but they are most likely in SI-units, because a corresponding magnetite content of 30-40 % in the volcanics is highly unlikely. A log diagram of the 642E well in Schönharting & Abrahamsen (1989) supports this conclusion.

Site	Penetration	Number of samples	NRM (A/m)	Suscept. (SI)	Polarity	Mean inclination
338 ¹	437 m	7	3.1	0.016	Normal	70.4°
342 ¹	170 m	3	1.4	0.015	Reversed	-81.0°
642E ²	1229 m	221	5.0	0.030	Reversed	-63°

2.4 Bathymetric and topographic data

The bathymetry data for the deep-water part of the map come from satellite altimeter data released by Smith and Sandwell (1997). The bathymetric data from the shallow water areas were compiled by The Norwegian Mapping Authority, Marine Department in Stavanger. This data set has three different sources; 1) modern multi-beam echo sounder in the Vestfjorden area, 2) digitised naval maps in areas adjacent to the coast and 3) depth data collected during seismic surveys in areas further offshore. The quality of these data varies considerably. Data set 1 has the highest quality while data set 3 is poorest. The cell size of the combined grid is 1 km x 1 km.

Very coarse data to fill in the gaps in coverage were extracted from a global data set supplied with the ER-Mapper software. High-resolution topography data (100m x 100m) for Norway were supplied by the Norwegian Mapping Authority. Topography for Sweden was downloaded from the GTOPO30 data set (<http://edcwww.cr.usgs.gov/landdaac/gtopo30/gtopo30.html>). The final grid shown in Fig. 1 was displayed using the shaded-relief technique with illumination from the southeast. The grey tone part of the maps is calculated from a 20 km high pass filtered grid and is superimposed on the coloured elevation model.

3 INTERPRETATION METHODS

3.1 Interpretation of depth to anomaly sources

Depths to basement have been estimated from inversion of aeromagnetic and gravity data, applying the autocorrelation algorithm of Phillips (1979), the 3D Euler deconvolution algorithm of Reid *et al.* (1990) and a least-squares optimising algorithm of Murthy & Rao (1989). The autocorrelation method is assuming that the magnetic basement is defined as a two-dimensional (2D) surface constructed from a large number of thin vertical 'dykes' of differing magnetisation. The upper terminations of the 'dykes' define the basement surface. The depth to this surface is estimated by passing a short window along the magnetic profile, estimating a depth for each position of the window. A total of 611 autocorrelation depth estimates are plotted on Fig. 9. The method has the advantage that sources at different depths can be separated, i.e. anomalies caused by deep and shallow bodies in the same profile. This is especially useful in the western Lofoten area where abundant lava flows/sills occur within the sedimentary sequence.

The Euler 3-D deconvolution (Reid *et al.* 1990, Geosoft 2000b) was also used to estimate the depth to magnetic basement rocks assuming the magnetic anomalies caused by a faulted basement. A structural index (SI) of 0.5 (thick step) was applied because this index gave the most focused depth estimates in the eastern platform area. A structural index of 1 (sill/dyke) seems, however, to be more appropriate in parts of the western area where the flow basalts/sills occur. The number of solutions (SI=0.5) was reduced using two different filtering techniques. Unreliable solutions with large distance from sources and large standard deviation were first removed using the filtering technique provided by the software vendor (Geosoft 2000b). A median filter (described by Olesen & Smethurst 1995) - which removes data in dense areas only - was subsequently applied. Outlying data are removed until the number of depth estimates per square kilometre falls to a user specified limit (1 estimate per 200 km²). The first step of filtering reduced the number of solutions from 147.000 to 34.700 solutions while the second step brought it down to 403. The estimates are plotted in Figs. 9 & 12.

The 2D magnetic depth estimates and gravity inversion profiles have been reported earlier by Olesen & Torsvik (1993). A combined depth-to-basement map has been constructed from the magnetic and gravity depth estimates. In areas where the gravity and magnetic datasets give diverging depth estimates the gravity interpretation is given highest priority, especially in areas where we expect to find shallow, low-magnetic basement continuing from onshore areas or as a result of down-faulted Caledonian nappes or amphibolite facies gneisses within the deep basins. High frequency anomalies interpreted to represent magnetic volcanics were excluded in the contouring.

Fault zones within the basement and partly within the sediments were interpreted from the geophysical images. High gravity gradients along the basin boundaries are generally interpreted to be caused by faults but may in some cases be related to steeply dipping sedimentary bedding.

An Airy-Heiskanen 'root' (Heiskanen & Moritz 1967) was calculated from the compiled topographic and bathymetric data-set. The gravitational attraction from the 'root' was calculated using the AIRYROOT algorithm (Simpson *et al.* 1983). The isostatic residual (Fig. 7) was achieved by subtracting the gravity response of the Airy-Heiskanen 'root' from the observed Bouguer gravity data.

3.2 Image enhancements

The separation of the residual field on the magnetic and gravity datasets is carried out in the frequency domain using 8 and 100 km Gaussian filters, respectively. Shaded relief versions in black/white of the high pass filtered datasets are superimposed on the coloured total field (Figs. 6 & 8). The colour maps are presented with a histogram equalising technique, i.e. each colour cover the same area on the map.

The grid data-sets were analysed with the Oasis Montaj software (Geosoft 2000c, 2001). Histogram-equalised colour, high-frequency filtered and shaded-relief images have been used to enhance the information of the regional data-sets. Shaded-relief presentations, which treat the grid as topography illuminated from a particular direction, have the property of enhancing features which do not trend parallel to the direction of illumination. These images proved especially useful for mapping of the fault zones within the survey area.

The shaded-relief of the aeromagnetic and gravity grids are shown in Figs. 5 - 8. The 'illumination' is from the SE. The sedimentary sub-crop pattern (Rokoengen *et al.* 1988, Løseth & Fanavoll 1992) is plotted on Fig. 6 for comparison with the high-frequency magnetic anomalies.

3.3 GM-SYS interactive modelling

I have carried out forward modelling of the gravity and magnetic fields along two seismic profiles across the Lofoten margin (Figs. 1-12). Profile A-A' is composed of four line segments (Table 7) while profile B-B' constitutes a single seismic line (RHW96-110, shot point 101-3079, from UTM 520809- 7544148 to UTM 580439- 749958m, zone 32). When computing the response from the model I have used the GM-SYS computer program from Northwest Geophysical Associates (2000). The basic model in this program comprises 2½ dimensional bodies, i.e. bodies of polygonal cross-section of finite length in the strike direction.

Constraints offered by seismic interpretations provided by Tom Bugge and Peter Midbøe (pers.

comm. 2001) have been used. The seismic interpretations were depth-converted using well-data and interval stacking velocities from seismic sections (Table 5). The depth-converted seismic horizons were imported directly into the GM-SYS programme package. The depth estimates obtained from the autocorrelation and Euler methods was also used to constrain the models. Applied density estimates of sediments and basement are shown in Table 4 while published magnetic properties of volcanic rocks in the Vøring area are displayed in Table 6. The Moho topography and lower crustal densities have been deduced from published OBS seismic data (Mjelde et al. 1992, 1993, 1998). I present three alternative models for profile A-A' and two models for profile B-B'.

Table 7. Profile segments in composite line A-A'.

Line	Start shot point	Stop shot point	Start UTM coord. (UTM zone	Stop UTM coord. 32)
VB-26-89	3580	906	464966	7501038 531096 7510653
RHW96-506	1271	2545	531257	7510675 563104 7511231
N6-92-107	211	3056	563129	7511235 600615 7484379
TB-48-87	1416	805	602615	7481346 615030 7472448

3.4 Geophysical interpretation map

Fault zones within the basement and partly within the sediments are interpreted from the aeromagnetic map. The fault zones are characterized by (Henkel 1991, Henkel & Guzmán 1977):

1. Linear discordances in the anomaly pattern.
2. Displacement of reference structures.
3. Linear gradients.
4. Discordant linear magnetic minima (only visible over shallow magnetic basement).

The faults are plotted on Figs. 2 & 9. High frequency anomalies representing volcanic rocks are also included. These anomalies are often negative. The combined interpretation of depth estimates from both gravity and aeromagnetic data has been carried out by interpolation and contouring of depth to basement. In areas where the two data sets give diverging depth estimates the gravity interpretation is given the highest weight, especially in areas where we expect to find low-magnetic basement continuing from onshore or down-faulted, amphibolite facies gneisses or Caledonian nappes within the deep basins. High frequency anomalies interpreted to represent magnetic volcanics are excluded in the contouring. All individual depth estimates from the gravity and aeromagnetic interpretation are plotted on the interpretation map (Figs 9 & 12).

4 STRUCTURAL FRAMEWORK

The area offshore the Lofoten and Vesterålen Islands is characterized by several fault-bounded basins and highs (Eldholm *et al.* 1979, Blystad *et al.* 1995). The major structural elements are shown on Fig. 2. The structure names are adapted from Blystad *et al.* (1995), Løseth & Tveten (1996) and Olesen *et al.* (1997). Some major fault structures and a major volcanic complex (Myken) interpreted from the present aeromagnetic and gravity data have been added to the map. The major features include a structural high, the Utrøst Ridge, on the landward side of the shelf edge and a basinal area, the Ribban Basin, on the inner shelf. The Røst High and the Jennegga High occur to the south and to the north, respectively, on the Utrøst Ridge. The Skomvær and Havbåen Subbasins are situated within the Ribban Basin. The Marmæle Spur is situated to the west of the Skomvær Subbasin. The seaward boundary of the Utrøst Ridge has large faults (Mokhtari & Pegrum 1992, Mjelde *et al.* 1992) with northwest throws and forms the landward boundary of the Røst Basin which is covered by a sequence of basalt flows. The evidence of a sub-basalt sedimentary sequence is based on data derived from inversion of gravity data (Sellevoll *et al.* 1988), ocean bottom seismographs (Mjelde *et al.* 1992) and forward gravity modelling (Olesen *et al.* 1997).

The basement in the Lofoten-Senja area is dominated by Precambrian high-grade migmatitic gneisses and intrusives, of intermediate composition to the south and granitoid composition to the north (Griffin *et al.* 1978, Tveten 1978). The shallow Moho discontinuity (Sellevoll 1983) in the area is most likely formed caused during a Cretaceous rift phase. The exhumation of the deep-crustal rocks in the Lofoten has also lately been related to the formation of core complex in the Permian (Hames & Andresen 1996). Gaal & Gorbatshev (1987) have interpreted the intrusive rocks in the Lofoten-Ringvassøya basement area and the Høgtuva-Sjona and Saltfjellet tectonic windows to be an integral part of the Transscandinavian Granite-Porphry Belt (TGPB), which continues to the south and east beneath the Caledonides into Sweden. The belt of Proterozoic intrusives extends to southern Sweden and is characterised by regional magnetic anomalies. To the west of the TGPB lies the Protogine Zone (PZ) which is a continental scale zone of deformation reactivated several times during the Proterozoic. This zone is trending in a N-S direction below the Caledonian Nappes in Nordland (Olesen *et al.* 1997). The Nesna Shear Zone (Osmundsen *et al.* 2000) and the Bivrost Lineament (Blystad *et al.* 1995) may constitute the extension of the Protogine Zone onto the continental shelf, and may therefore represent rejuvenation of a much older zone of crustal weakness as also suggested by Mokhtari & Pegrum (1992). Downfaulted low-magnetic Caledonian nappes may constitute the basement to the southwest of the Bivrost Lineament. Two NNW-SSE oriented oceanic transform zones extend into the survey area: the Bivrost and Jennegga Fracture Zones. The Senja Fracture Zone is located immediately to the north of the survey area.

A crustal scale shear zone occurs within the Precambrian basement in Troms. The Bothnian-Senja shear zone (Henkel 1991, Zwaan 1995 and Olesen *et al.* 1997) can be observed on Senja and Kvaløya on either side of Malangen. A prominent set of high-angle semi-ductile to cataclastic faults called the Vestfjorden-Vanna fault complex (Andresen & Forslund 1987) continues from the

Vestfjorden area through the sounds to the east of Hinnøya, Senja and Kvaløya. The fault complex constitutes the contact between the Precambrian terrain to the west and the Caledonian nappe sequence to the east. There is evidence of both Late Paleozoic and Mesozoic activity along the fault complex (Andresen & Forslund 1987, Olesen *et al.* 1997). The NE-SW trending 'Heier Zone' on Langøya (Løseth & Tveten 1996) and the Nesna shear zone in the Rana Area (Osmundsen *et al.* 2000) are mainland candidates for late Caledonian detachments.

The northern Scandinavian dome of Plio-Pleistocene age (Riis 1996) is one of several domes in the circum-Atlantic area. The dome is partly situated on the continental shelf (Lofoten-Vesterålen and Vestfjorden area) and partly on land (Saltfjellet-Tysfjord-Sarek area). This mechanism has contributed to the exhumation of deep-seated crustal rocks in the Lofoten-Vesterålen area.

5 RESULTS

5.1 Regional basement configuration - transfer zones

The long-wavelength component of the offshore gravity field is partly interpreted in terms of a Moho topography as shown by Sellevoll (1983) and Olesen *et al.* (1997). A Moho bulge occurs in the Lofoten-Vesterålen area. A similar Moho bulge occurs below the Utgard High/Træna Basin (Planke *et al.* 1991, Skogseid *et al.* 1992, Olesen & Smethurst 1995). The Jurassic to Early Cretaceous rift axis is located along the Træna, Ribban, Vestfjorden and Harstad Basins that are all underlain by a shallow Moho. The individual segments of the master faults along the rift are connected by transfer zones (Olesen *et al.* 1997). Several shifts in the polarity of faults occur along the continuation of this Mid-Norwegian rift-terrain into the Lofoten-Senja area (Fig. 7). These zones are diagnostic for continental rifting and occur as two different types: (1) transverse faults e.g. the Lenvik transfer zone or (2) twist zones (Colletta *et al.* 1988) e.g. the Vesterålen transfer zone. The former is bounded by steeply dipping transverse faults inherited from old weakness zones along the Bothnian-Senja fault complex, while no major transverse fault seems to occur within the latter. I also suggest that the Bivrost Lineament constitutes a transfer zone because of the shifts in polarity of the main faults across this zone. This zone may represent a reactivation of the Precambrian Protogine zone along the western margin of the Transscandinavian Granite-Porphry Belt (Larson *et al.* 1990) and the Devonian Nesna shear zone (Osmundsen *et al.* 2000). The spacing between the regional transfer zones is 120-140 km.

The Mosken and Melbu transfer zones occur on a local scale and do not trend across the whole paleo-rift structure. The Mosken transfer zone is located between Moskenesøy and Værøy in the southwestern part of Lofoten. This transfer zone separates the two parts of the Vestfjorden Basin with opposing polarity; the northeastern subbasin with the master-fault to the southwest (towards

Hamarøya) and the southwestern subbasin with the master-fault along the Lofoten Ridge. The latter transfer zone is most likely a twist-zone similar to the Vesterålen transfer zone. The Melbu transfer zone (Figs. 2 & 9) separates the southeast facing faults to the east of the Jenegga High from the northwest facing masterfault in the Havbåen Subbasin. The Melbu transfer zone does not continue across the Lofoten Ridge to Vestfjorden.

Three well known transform faults within the oceanic crust continue into the survey area; i.e. the Bivrost, Jenegga and Senja fracture zones. The regional transfer zones, Bivrost, Vesterålen and Lenvik, extend into these oceanic fracture zones indicating that these Cenozoic structures follow older NW-SE trending zones of weakness. Changes in Moho depths occur locally along the Bivrost and Vesterålen transfer zones indicating that these zones extend through the whole crust.

5.2 Sandflesa Area

The western part of interpretation profile A-A' intersects a coinciding gravity and aeromagnetic anomaly located between the Utgard High and the Røst High (Figs. 5-8). The magnetic anomaly is restricted to a smaller area than the gravimetric one. A substantial excess of mass must occur in the crystalline basement and/or the sedimentary sequence to cause one of the largest observed gravity anomalies (90 mGal) on the Mid-Norwegian continental shelf. There is in addition a shallow Moho (22 km) in this area (Mjelde *et al.* 1998). The depth to the magnetic sources is approximately 3 km (Figs. 9 & 12). I conclude that the gravity and magnetic anomalies may be related to one or more of the following three models: (a) mafic volcanic intrusions, (b) a basement high or (c) a thick sequence of volcanic rocks. These models are illustrated in Figs. 13-22. I favour interpretation (a) (Figs. 13-14) because Mjelde *et al.* (1998) have reported intermediate seismic velocities (4-5 km/s) at a depth of 7 km in this area. I envisage a complex mixture of volcanics and sediments within this volcanic centre as illustrated in the presented model (Figs. 13-14). (Note that the potential field data alone cannot resolve details within the complex.) A shallow basement (model b, Figs. 15-16) at a depth of c. 3 km is less likely because of the intermediate seismic velocities in the depth interval 3-7 km. The 2.5 km thick volcanic sequence (model c, Fig. 17-18) located at a depth of 2.5-5.0 km is also less likely since the underlying sediments have an anomalous high velocity. Berndt *et al.* (2001) have interpreted a gently dipping, strong reflector in terms of a tuff sheet in the Sandflesa area. An alternative interpretation is an erosional surface in sub-aerial volcanics. I suggest applying the name Myken (from one of the outermost islands on the Helgeland coast) to the volcanic complex. A possible cauldron complex (Lundin *et al.* in press) is located within the Hel Graben immediately to the southwest of the Myken complex. The Hel Graben has earlier been interpreted to be a centre of igneous activity on the basis of seismic velocities (Berndt *et al.* 2000). Our interpretation suggests that a basement high (Sandflesa High) is situated below the volcanic complex which is also consistent with earlier interpretations by Olesen *et al.* (1997) and Mjelde *et al.* (1998). The age of the intrusions is uncertain but a late Cretaceous-Early Tertiary age is likely because the area is

located adjacent to the Vøring volcanic province. This volcanic complex may resemble the seamounts or 'hot points' occurring as intrusive (dolerite/gabbro/peridotite/gneiss) complexes in the Red Sea (Bonatti & Seyler 1987, Cochran & Martinez 1988). Lundin & Doré (1997) have interpreted similar seamounts in the Rockall Trough and the Faeroe-Shetland Basin. These intrusive complexes are mostly of Palaeocene age (Stoker et al. 1993).

The gradient of the gravity field is highest on the eastern flank of the Sandflesa anomaly indicating a boundary fault to the east (Figs. 7, 8 & 9). The basement in the Utgard High to the south of the Sandflesa area is located at a depth of c. 6 km while the Træna Basin is 10-12 km deep. The shallow depth estimates along the Nyk High to the southwest show that the corresponding magnetic anomaly is caused by the termination of reversed magnetised sills towards the structural high rather than magnetic basement rocks below.

The depth to the basement in the Røst Basin, which is covered by a thick layer of volcanics, is c. 9 km (Olesen *et al.* 1997). The ocean/continent boundary is displayed on the interpretation map (Fig. 9) but is not well defined on the gravity and aeromagnetic maps indicating an 'oceanisation' of the continental crust along a transition between the two crustal types. The bulk of the magnetic rocks in the Sandflesa area and Røst Basin represent volcanics since the depths are shallower than basement depths obtained from seismic data and gravity modelling. Some of the depth estimates along the Utrøst Ridge do on the other hand represent depth to magnetic sources within the basement, i.e. below the basement surface. The occurrence of low-magnetic basement is also evident from the modelling of both profile A-A' and B-B' (Figs. 12-22). Rotated fault-blocks have been interpreted on multichannel seismic data to the west of the large-scale faults along the seaward boundary of the Utrøst Ridge. Profile B-B' cuts across the northeastern extension of the Sandflesa anomaly. I suggest two alternative models to explain the positive gravity anomaly along the profile: (a) Mafic intrusions in or near the uppermost basement (b) Mafic intrusions in the deeper crust (which may represent magmatic underplating). Both models can explain the observed anomaly. The continuation of the gravity anomaly from the Myken Volcanic Complex/Sandflesa High does, however, indicate that there may also be shallow intrusions in the uppermost crust below profile B-B'. But it is not possible from the potential data alone to decide which of these two models is the most correct.

5.3 Lofoten – Vesterålen area

The Ribban basin area is characterized by large depths to the magnetic basement. The largest depths, up to 10 km, correspond to the Skomvær and Havbåen Subbasins within the Ribban Basin. Modelling of gravity data give much shallower depths (up to 5 km). I interpret this discrepancy to be caused by downfaulted low-magnetic Caledonian nappes or low-magnetic amphibolite-facies gneisses. Previous potential field studies in the areas have arrived upon similar conclusions (Åm 1975, Olesen *et al.* 1997, Norsk Hydro 1998). The occurrence of low-magnetic basement is illustrated on the interpretation profiles (A-A' and B-B'). The Skomvær Basin is a half-graben bordered by a steep fault towards the Lofoten Islands. A shallow basement ridge at 1-3 km depth between the Røst High and the Skomvær Subbasin corresponds with the Marmæle Spur. However, large depths to basement (c. 4 km, Fig. 9) are obtained from both gravity and magnetic data to the north of the Marmæle Spur, which are significantly different from the depths interpreted from multichannel seismics, indicating that there may be an approximately 2 km thick sequence of low-density sediments below the base-Cretaceous in this area. The quality of the multichannel reflection seismic data is poor in this particular area due to pronounced seafloor multiples.

The southern part of the Vestfjorden Basin is a 7 - 8 km deep half graben defined by a boundary fault along the western margin as also shown by Brekke & Riis (1987). The northern part of the Vestfjorden Basin, however, is a shallower (approximately 2 km deep) half graben with the boundary fault along the eastern margin of the basin (Olesen *et al.* 1997). I suggest the name Hamarøya Fault Zone for this major structure. The Mosken transfer zone is separating the areas with opposing fault throw. From the aeromagnetic maps I interpret the western margin in the Lødingen area to consist of several rotated fault blocks extending from Austvågøya and Hinnøya into the Vestfjorden Basin. Raftsundet and Øksfjorden have very conspicuous topographic and bathymetric expressions and coincide with negative magnetic anomalies that are located between the rotated, magnetic fault blocks. These fjords and sounds contain most likely the fault zones separating the rotated fault blocks.

The uplift of the Vesterålen area is of a more dome-like character compared with the typical horst structure of the Lofoten Islands. The offshore basement-faults are also less distinct and the vertical offsets along them are smaller. The Harstad Basin is, however, more than 7 km deep to the west of Andøya. This depth has been interpreted from gravity data (Olesen *et al.* 1997). All the depth estimates from the aeromagnetic interpretation are shallower, but these depths do, however, most likely represent depth to magnetic volcanics. The magnetic anomalies at the eastern margin of the basin are continuous from the Vesterålen islands and most likely reflect rotated blocks within the basement. The NE-SW trending high frequency anomalies in this area represent volcanic rocks. The easternmost anomalies occur along a zone coinciding with the shelf edge and most likely represent the easternmost limit of the flow-basalts. The interpreted depths to these anomalies are in the order of 0.5 - 2.0 km below sea level.

5.4 Neogene uplift

Isostatically-corrected Bouguer gravity data from northwestern Fennoscandia reveal a round, 200 km wide negative anomaly situated in the area between Saltfjellet, Sarek, Vestfjorden and Ofotfjorden (Fig. 7). The anomaly is situated immediately to the east of the Lofoten-Vesterålen positive gravity anomaly and includes the area with the highest mountains in northern Scandinavia. The amplitudes of the negative and positive anomalies are -60 and +100 mGal, respectively.

The negative Sarek-Vestfjorden anomaly can be explained by a low-density mantle (Olesen 2000). This hypothesis is supported by the low P- and S-wave velocities found in the mantle below the mountainous area of Scandinavia (Bannister *et al.* 1991). The large wavelength of the Sarek-Vestfjorden anomaly indicates that the source is deep-seated. The Lofoten-Vestfjorden-Sarek region is mainly in isostatic equilibrium due to the opposing effects of the positive and negative gravity anomalies. The buoyancy of the low-density mantle below the Sarek-Vestfjorden area has, in other words, caused the Neogene uplift of the area and is still keeping the Lofoten-Vesterålen area in an elevated position despite the dense and thin crust of the latter area. The area may have experienced an additional uplift due to the isostatic effect of the erosional unloading of the exposed soft sediments. This model is consistent with the mantle convection and asthenospheric diapirism models proposed by Stuevold *et al.* (1992) and Rohrman & van den Beek (1996).

5.5 Internal basin structures

The compilation of modern aeromagnetic surveys (LAS-89, NAS-94, VAS-98 and HRAMS-97/98) has revealed several sets of high frequency anomalies. Low-amplitude and short-wavelength anomalies, often superimposed on long wave-length anomalies, are caused by magnetic sources within the sedimentary sequences in the southeastern part of the survey area. (Fig. 6). The bulk of this anomaly pattern is caused by magnetic sedimentary rocks of Quaternary age and Mesozoic-Tertiary sub-cropping sedimentary units. The asymmetry of the anomalies – with a steep gradient and a negative anomaly to the east and a more gentle gradient to the west (Olesen & Smethurst 1995) shows that the latter sources of the anomalies dip gently towards the west, consistent with interpretations of seismic data (Rokoengen *et al.* 1988). The most distinct of the anomalies represents 'unit IX' (see Fig. 6) on the IKU bedrock geology map of the Mid Norwegian Shelf (Rokoengen *et al.* 1988). The magnetic anomalies related to this early Oligocene 'unit IX' are most pronounced in the Helgeland area to the south of the present study area (see Fig. 17.4-17.5 in Olesen 2000). The magnetic anomalies associated with Quaternary overburden can be distinguished from the sub-crop anomalies since they do not show the pronounced asymmetrical shape. Some of the high-frequency magnetic anomalies in Vestfjorden originate from moraine ridges and other

Quaternary sediment units. The sub-crop units in the Lofoten-Vesterålen area do not cause the same distinct set of anomalies as along the coast of Helgeland. This is evident when superimposing the digitised subcrop map by Løseth & Fanavoll (1992) on top of the high-pass filtered aeromagnetic map (Fig. 6). This may partly be due to the lower sensitivity of the old caesium vapour magnetometer used in the LAS-89 survey compared with the modern caesium instrument applied in the NAS-94 survey. Some of the high-frequency anomalies related to moraine ridges in an area covered by both the LAS-89 and NAS-94 surveys (Fig. 3) are, however, visible on both surveys. A low magnetic susceptibility of the sediments in the Lofoten area may therefore also be an explanation for this difference in magnetic anomaly pattern. Occurrence of detrital Fe-Ti oxides and diagenetic siderite cement are the main magnetic source within the sediments in the Nordland area (Mørk & Olesen 1995). There may, for instance, be a lower content of siderite or Fe-Ti oxides in the sediments in the Ribban and Vestfjorden Basins compared to the sediments on Trøndelag Platform.

High frequency anomalies, representing potential volcanic rocks, are also indicated in the interpretation map (Figs. 9 & 12). They occur in a continuous zone from the western margin of the Utgard High northwards along the shelf edge to the west of the Utrøst Ridge up to Andøya (Fig. 6). They often show negative anomalies, which suggest that they represent flow basalts, and/or sills, which locally may be quite thick (in the order of kilometres).

6 CONCLUSIONS

1. The Lofoten area constitutes an extension of the Mid-Norwegian Permian and late Jurassic rifts which have been exhumed due to Permian and late Cretaceous-Paleogene rift-flank uplift and Plio-Pleistocene doming. The rifting events have resulted in a shallow Moho, uplifted core complexes and rotated basement-blocks separated by transfer zones. The Bivrost, Mosken, Melbu, Vesterålen and Lenvik transfer zones are located where shifts in polarity occur along the faults and separate individual rotated fault blocks. This is most noticeable in the Ribban and Vestfjorden Basins but can also be observed further to the northeast along the Vestfjorden-Vanna fault complex. Changes in Moho depths occur across the Bivrost and Vesterålen transfer zones indicating that these structures are continuous through the whole crust.
2. The combined interpretation of depth to basement reveals a depth of 5 km in the Ribban Basin offshore Lofoten and 9 km in the Røst Basin. Greater depths to magnetic basement occur locally. I interpret these most likely to represent down-faulted Caledonian nappes, Devonian sediments or low-magnetic (amphibolite facies) Precambrian rocks.
3. A substantial excess of mass must occur in the crust to cause the observed large gravity anomaly (90 mGal) in the Sandflesa area. When taking into account existing seismic information, I conclude

that the gravity and magnetic anomalies are most likely caused by large mafic intrusions in both the basement and the overlying sediments. There is most likely a complex mixture of volcanics and sediments within this volcanic centre. Rotated fault blocks situated between the Røst Basin and Utrøst Ridge immediately to the northeast of the Sandflesa area do also contain dense rocks, most likely mafic intrusions. The depth extent and age of these rocks can, however, not be resolved from the potential field data. A late Cretaceous-Early Tertiary age is, however, likely because the area is located adjacent to the Vøring volcanic province.

4. The aeromagnetic data show that the Precambrian intrusive rocks in the Lofoten-Senja basement complex are continuous below the Vestfjorden Basin and the Caledonian nappes to the tectonic windows in Nordland and further into Sweden and constitute part of the Transscandinavian Granite-Porphyry Belt. Several basement faults on the continental shelf can be traced onto the mainland. Reactivation of old shear zones is commonly observed. The Senja Fracture Zone and the Lenvik transfer zone are reactivations of the Proterozoic Bothnian-Senja fault complex while the Bivrost transfer zone (lineament) could represent a rejuvenation of the Proterozoic Protogine Zone and the Devonian Nesna shear zone.

5. A round, 200 km wide negative anomaly in the isostatically corrected Bouguer gravity data-set occurs in the Sarek-Vestfjorden area immediately to the east of the Lofoten-Vesterålen positive gravity anomaly. Both the negative gravity anomaly and the Neogene uplift of the region could be caused by a low-density material within the mantle. The Lofoten-Vestfjorden-Sarek region may be in isostatic equilibrium due to the opposing effects of the positive and negative gravity anomalies.

6. The high-frequency anomaly pattern evident in the compilation of modern high-resolution surveys is interpreted to have three different types of magnetic sources; a) Quaternary overburden of varying thickness and bathymetric features, b) sub-cropping sedimentary units, c) Flow basalts and sills, notably along the western margin of the Utgard High and Utrøst Ridge up to Andøya.

7 RECOMMENDATIONS FOR FURTHER WORK

1. Most of the Sandflesa area is covered with rather old aeromagnetic data (from 1973). There has been a substantial development of both instruments and navigation systems during the last 30 years. I do therefore recommend acquiring a new aeromagnetic survey in this area.
2. More recent gravity surveys in the Nordland VI-VII area should be included and levelled with the existing gravity lines to improve the data coverage in the area.
3. I also recommend a compilation of density data from exploration wells in Nordland IV and adjacent areas.
4. I have used a modelling package (GM-SYS) assuming 2½ dimensional bodies, i.e. bodies of polygonal cross-section of finite length in the strike direction. A full 3D modelling of the complex anomalies in the Sandflesa could, however, provide a more detailed shape of the intrusive bodies. Modelling of gradients and/or wavelength filtered residuals should also be tested. I have modelled the Free air gravity and total field magnetic data in the present study and tried to fit both the amplitudes and gradients of the calculated field to the observed field.
5. A combined interpretation of the Lofoten-Vøring and East-Greenland conjugate margins would improve the understanding of the pre-drift tectonic development of both areas.

8 ACKNOWLEDGEMENTS

Tom Bugge, Kate Langaker and Peter Midbøe in Norsk Hydro provided seismic interpretations for the integrated interpretations and contributed with stimulating discussions. Jomar Gellein digitised the IKU bedrock map from the Nordland VI and VII area. Erik Lundin, NGU provided important information on the volcanic activity in the north Atlantic area. Section leader Mark A. Smethurst carried out the quality control of the present report.

9 REFERENCES

- Andersen, O.B. & Knudsen, P. 1998: Gravity anomalies derived from the ERS-1 satellite altimetry. Kort og Matrikelstyrelsen, DK-2400 Copenhagen NV, Denmark (www.kms.dk).
- Andresen, A. & Forslund, T. 1987: Post-Caledonian brittle faults in Troms: geometry, age and tectonic significance. *The Caledonian and related geology of Scandinavia* (Cardiff, 22-23 Sept., 1989) (Conf. abstr.).
- Bannister, S.C., Ruud, B.O. & Husebye, E.S. 1991: Tomographic estimates of sub-Moho seismic velocities in Fennoscandia and structural implications. *Tectonophysics* 189, 37-53.
- Berndt, C., Skogly, O.P., Planke, S., Eldholm, O., Mjelde, R. 2000: High-velocity breakup-related sills in the Voring Basin, off Norway. *Journ. Geophys. Research* 105, 28.443-28.454.
- Berndt, C., Planke, S., Alvestad, E., Tsikalas, F. & Rasmussen, T. 2001: Seismic volcanostratigraphy of the Norwegian Margin: constraints on tectonomagmatic break-up processes. *Journ. Geol. Soc. London* 158, 413-426.
- Blystad, P., Brekke, H., Færseth, R.B., Larsen, B.T., Skogseid, J. & Tørudbakken, B. 1995: Structural elements of the Norwegian continental shelf, Part II. The Norwegian Sea Region. *Nor. Petr. Dir. Bull.* 8, 45 pp.
- Bonatti, E. & Seyler, M. 1987: Crustal underplating and evolution in the Red Sea Rift: uplifted gabbro/gneiss complexes on Zabargad and Brothers islands. *Journ. Geophys. Research* 92, 12.803-12.821.
- Brekke, H. & Riis, F. 1987: Tectonics and basin evolution of the Norwegian shelf between 62° and 72°N. *Nor. Geol. Tidsskr.* 67, 295-322.
- Cochran, J.R. & Martinez, F. 1988: Evidence from the northern Red Sea on the transition from continental to oceanic rifting. *Tectonophysics* 153, 25-53.
- Colletta, B., Le Quellec, Letouzey, P. & Moretti, I. 1988: Longitudinal evolution of the Suez rift structure (Egypt). In X. Le Pichon & J.R. Cochran (eds.), *The Gulf of Suez and Red Sea Rifting*. *Tectonophysics* 153, 221-233.
- Eldholm, O., Sundvor, E. & Myhre, A. 1979: Continental margin off Lofoten-Vesterålen, Northern Norway. *Marine Geophys. Res.* 4, 3-35.
- Eldholm, O., Thiede, J. & Taylor, E. et al. (Eds.) 1987: Proc. ODP, Initial Reports 104, College Station, TX (Ocean Drilling Program).
- Eldholm, O., Thiede, J. & Taylor, E. and shipboard scientific party 1987: Summary and preliminary conclusions, ODP leg 104. In Eldholm, O., Thiede, J. & Taylor, E. et al. Proc. ODP, Initial Reports 104, 751-771.
- Gaal, G. & Gorbatshev, R. 1987: An outline of the Precambrian evolution of the Baltic Shield. *Precambrian Research* 35, 15-52.
- Geosoft 2001: OASIS Montaj v 5.1, The core software platform for working with large volume spatial data. Quick start tutorials. Data Processing System for Earth Sciences Applications. Users manual. 228 pp.

- Geosoft 2000a: Geosoft GridKnit, Grid stitching tool for OASIS montaj, Tutorial and user guide, 28 pp.
- Geosoft 2000b: Euler 3-D Deconvolution (Euler_{3D}), Processing, analysis and visualization system for 3D inversion of potential field data., Tutorial and user guide, 58 pp.
- Geosoft 2000c: MAGMAP (2D-FFT), 2-D frequency domain processing of potential field data. Tutorial, 67 pp.
- Griffin, W.L., Taylor, P.N., Hakkinen, J.W., Heier, K.S., Iden, I.K., Krogh, E.J., Malm, O., Olsen, K.I., Ormaasen, D.E. & Tveten, E. 1978: Archean and Proterozoic crustal evolution in Lofoten-Vesterålen, North Norway. *J. Geol. Soc. London* 135, 629-647.
- Hames, W.E. & Andresen, A. 1996: Timing of Paleozoic orogeny and extension in the continental shelf of north-central Norway as indicated by laser ⁴⁰Ar/³⁹Ar muscovite dating. *Geology* 24, 1005-1008.
- Heiskanen, W.A. & Moritz, H. 1967: Physical Geodesy. *W.H. Freeman, San Fransisco*. 364 pp.
- Henkel, H. 1991: Magnetic crustal structures in Northern Fennoscandia. In: P. Wasilewski & P. Hood (Eds.). Magnetic anomalies — land and sea. *Tectonophysics* 192, 57-79.
- Henkel, H. & Guzmán, M. 1977: Magnetic features of fracture zones. *Geoexploration* 15, 173-181.
- Kent, D.V. & Opdyke, N.D. 1978: Paleomagnetism and magnetic properties of igneous rock samples – Leg 38. In Talwani, Udintsev *et al.* (Eds.) Initial reports of the Deep Sea Drilling Project, Supplements to Vol. 38, 39, 40 and 41. *Govt. Printing Office, Washington, D.C.*, 3-8.
- Larson, S.Å., Berglund, J., Stigh, J. & Tullborg, E.-L. 1990: The Protogine Zone, southwest Sweden: a new model - an old issue. In Gower, C.F., Rivers, T. & Ryan, B. (eds.) *Mid-Proterozoic Laurentia-Baltica*, 317-333. Geological Association of Canada, Special Paper 38.
- Lundin, E.R., Rønning, K., Doré, A.G. & Olesen O. in press: Hel Graben, Vøring Basin, Norway – a possible major cauldron? Abstract, 25th Nordic Geological Winter Meeting, January 6th - 9th, 2002, Reykjavik.
- Lundin, E.R., Doré, A.G. 1997: A tectonic modell for the Norwegian passive margin with implications for the NE Atlantic: Early Cretaceous to break-up. *Journ. Geol. Soc. London* 1584 545-550.
- Løseth, H. & Fanavoll, S. 1992: Bedrock geology map Norwegian shelf 67° - 69°30'N. In: Shallow drilling Nordland VI and VII 1991. IKU Report 23.1594.00/02/92.
- Løseth, H. & Tveten, E., 1996: Post-Caledonian structural evolution of the Lofoten and Vesterålen offshore and onshore areas. *Norsk Geologisk Tidsskrift* 76.
- Mathisen, O. 1976: A method for Bouguer reduction with rapid calculation of terrain corrections. *Geographical Survey of Norway geodetic publications* 18, 40 pp.
- Martinez, F. & Cochran, J.R. 1988: Structure and tectonics of the northern Red Sea: catching a continental margin between rifting and drifting. *Tectonophysics* 150, 1-32.
- Mauring, E., Beard, L.P., Kihle, O. & Smethurst, M.A. in press: A comparison of aeromagnetic levelling techniques with an introduction to median levelling. *Geophysical Prospecting*
- Mjelde, R., Sellevoll, M.A., Shimamura, H., Iwasaki, T. and Kanazawa, T. 1992: A crustal study

- off Lofoten, N.Norway, by use of 3-component ocean bottom seismographs. *Tectonophysics* 212, 269-288.
- Mjelde, R., Sellevoll, M.A., Shimamura, H., Iwasaki, T. and Kanazawa, T. 1993: Crustal structure beneath Lofoten, N.Norway, from vertical incidence and wide-angle seismic data. *Geophysical Journ. Int.* 114, 116-126.
- Mjelde, R., Digranes, P., Shimamura, H., Shiobara, H., Kodaira, S., Brekke, H., Egebjerg, T., Sørenes, N. & Thorbjørnsen, S. 1998: Crustal structure of the northern part of the Vøring Basin, mid-Norway margin, from wide-angle seismic and gravity data. *Tectonophysics* 293, 175-205.
- Mokhtari, M. & Pegrum, R.M. 1992: Structure and evolution of the Lofoten continental margin, offshore Norway. *Nor. Geol. Tidsskr.* 72, 339-355.
- Murthy, I.V.R. & Rao, S.J. 1989: Short note: A Fortran 77 program for inverting gravity anomalies of two-dimensional basement structures. *Computing & Geosciences* 15, 1149-1156.
- Mørk, M.B. & Olesen, O. 1995: Magnetic susceptibility of sedimentary rocks from shallow cores off Mid Norway and crystalline rocks from the adjacent onland areas. NAS-94 Interpretation Report, Part II: Petrophysical data. *NGU Report 95.039*, 68 pp
- Norges geologiske undersøkelse 1992: Aeromagnetisk anomalikart, Norge M 1:1 mill, Norges geologiske undersøkelse.
- Norsk Hydro 1998: Gravity and magnetic modeling in the Nordland VI area. Norsk Hydro Research Centre Internal Report, 9 pp.
- Northwest Geophysical Associates 2000: GM-SYS Gravity/Magnetic Modeling Software. User's Guide for version 4.6. 95 pp.
- Olesen, O. 2000: Regional structuring of the onshore-offshore Nordland area inferred from potential field data. In: Eide, E. 2000 (Ed.) *BAT Project 1998-2002 Technical Report 4 Status to December 2000*. 17.225-17.254.
- Olesen, O. & Torsvik, T.H. 1993: Interpretation of aeromagnetic and gravimetric data from the Lofoten-Lopphavet area. *NGU Report 93.032*, 77 pp
- Olesen, O., Torsvik, T.H., Tveten, E. & Zwaan, K.B. 1993: The Lofoten - Lopphavet Project, an integrated approach to the study of a passive continental margin, Summary report. *NGU Report 93.129*, 54 pp.
- Olesen, O., Henkel, H., Kaada, K. & Tveten, E. 1991: Petrophysical properties of a prograde amphibolite - granulite facies transition zone at Sigerfjord, Vesterålen, Northern Norway. In: P. Wasilewski & P. Hood (Eds.). *Magnetic anomalies — land and sea. Tectonophysics* 192, 33-39.
- Olesen, O. & Smethurst, M.A. 1995: NAS-94 Interpretation Report, Part III: Combined interpretation of aeromagnetic and gravity data. *NGU Report 95.040*, 50 pp.
- Olesen, O., Torsvik, T.H., Tveten, E., Zwaan, K.B., Løseth H. & Henningsen, T. 1997: Basement structure of the continental margin in the Lofoten-Lopphavet area, northern Norway: constraints from potential field data, on-land structural mapping and palaeomagnetic data. *Nor. Geol. Tidsskr.* 77, 15-33.

- Osmundsen, P.T., Braathen, A., Roberts, D. & Gjelle, S. 2000: Late- to Post-Caledonian tectonics in Mid Norway: The Nesna shear zone and its regional implications. Abstract 24th Nordic Geological Winter Meeting, Trondheim. p. 133.
- Phillips, J.D. 1979: ADEPT: A program to estimate depth to magnetic basement from sampled magnetic profiles. *U.S. geol. Surv. open-file report 79-367*, 35 pp.
- Planke, S., Skogseid, J. & Eldholm, O. 1991: Crustal structure off Norway, 62° to 70° north. *Tectonophysics 189*, 91-107.
- Reid, A.B., Allsop, J.M., Granser, H., Millett, A.J. & Sommerton, I.W. 1990: Magnetic interpretation in three dimensions using Euler deconvolution. *Geophysics 55*, 80-91.
- Riis, F. 1996: Quantification of Cenozoic vertical movements of Scandinavia by correlation of morphological surfaces with offshore data. *Global and Planetary Change 12*, 331-357.
- Rohrman, M. & van den Beek 1996: Cenozoic postrift domal uplift of North Atlantic margins: An asthenospheric diapirism model. *Geology 24*, 901-904.
- Rokoengen, K., Rise, L., Bugge, T. & Sættem, J. 1988: Bedrock geology of the Mid Norwegian Continental Shelf. Scale 1:1000 000. *IKU*
- Schlenger, C. M. 1985: Magnetization of lower crust and interpretation of regional magnetic anomalies: Example from Lofoten and Vesterålen, Norway. *J. Geophys. Res. 90*, 11484-11504.
- Schönharting, G. & Abrahamsen, N. 1989: Paleomagnetism of the volcanic sequence in hole 642E, ODP leg 104, Vøring Plateau, and correlation with early Tertiary basalts in the North Atlantic. In Eldholm, Thiede, Taylor *et al.* (Eds.) *Proceedings of the Ocean Drilling Program, Scientific Result 104*, College Station, TX, 911-920.
- Sellevoll, M.A. 1983: A study of the Earth in the island area of Lofoten- Vesterålen, northern Norway. *Nor. geol. unders. 380*, 235-243.
- Sellevoll, M.A., Olafsson, I., Mokhtari, M., Gidskehaug, A. 1988: Lofoten margin, North Norway: crustal structure adjacent to the ocean-continent transition. *Nor. geol. unders. Special Publ. 3*, 39-48.
- Simpson, R.W., Jachens, R.C., & Blakely, R.J. 1983: AIRYROOT: A Fortran program for calculating the gravitational attraction of an Airy isostatic root out to 166.7 km. *United States Department of the Interior, Geological Survey, Open-File Report 83-883*, 24 pp.
- Skogseid, J., Pedersen, T., and Larsen, V.B., 1992: Vøring Basin: subsidence and tectonic evolution. In Larsen, R.M., Brekke, H. Larsen, B.T. & Talleraas, E. (Eds.) *Structural and Tectonic Modelling and its Application to Petroleum Geology. NPF Special Publication, Elsevier, Amsterdam*, 55-82.
- Smith, W. H. F. & Sandwell, D. T. 1997: Global sea floor topography from satellite altimetry and ship depth soundings. *Science 277*, 1956-1962.
- Stoker, M.S., Hitchen, K. & Graham, C.C. 1993: Geology of the Hebrides and West Shetland shelves, and adjacent deep-water areas. United Kingdom offshore regional report, British Geological Survey. 149 pp.
- Stuevold, L.M., Skogseid, J. & Eldholm, O. 1992: Post-Cretaceous uplift events on the Vøring continental-margin. *Geology 20*, 919-922.

- Svela, P.T. 1971: Gravimetriske undersøkelser av Lofoten-Vesterålen området. *Unpubl. Cand. real. thesis, Univ. of Bergen*, 131 pp.
- Talwani, Udintsev *et al.* (Eds.) 1978: Initial reports of the Deep Sea Drilling Project, Supplements to Vol. 38, 39, 40 and 41. *Govt. Printing Office*, Washington, D.C.
- Tveten, E. 1978: Berggrunnsgeologisk kart Svolvær 1:250.000. *Norges geologiske undersøkelse, Trondheim*.
- Zwaan, K.B. 1995: Geology of the West Troms Basement Complex, northern Norway, with emphasis on the Senja Shear Belt: a preliminary account. *Norges geologiske undersøkelse Bull. 427*, 33-36.
- Åm, K. 1975: Aeromagnetic basement complex mapping north of latitude 62°N, Norway. *Nor. geol. unders. 316*, 351-374.

List of figures and tables

Figures

- Fig. 1. Shaded relief, bathymetry and topography, 100 and 500 m contour intervals.
- Fig. 2. Basement structures, Lofoten area.
- Fig. 3. Aeromagnetic database, Lofoten area.
- Fig. 4. Gravity database.
- Fig. 5. Total magnetic field referred to DGRF.
- Fig. 6. Gaussian 8km high-pass filtered magnetic field..
- Fig. 7. Isostatic residual, Bouguer gravity.
- Fig. 8. Gaussian 100 km high-pass filtered isostatic residual of Bouguer gravity.
- Fig. 9. Geophysical interpretation map, Lofoten area.
- Fig. 10. Total magnetic field referred to DGRF, Sandflesa area.
- Fig. 11. Isostatic residual of Bouguer gravity, Sandflesa area.
- Fig. 12. Geophysical interpretation map, Sandflesa area.
- Fig. 13. Modelling of aeromagnetic and gravity data along line A-A', alternative (a) mafic volcanic intrusions.
- Fig. 14. Modelling of aeromagnetic and gravity data along line A-A', alternative (a) mafic volcanic intrusions, uppermost 10 km.
- Fig. 15. Modelling of aeromagnetic and gravity data along line A-A', alternative (b) basement high.
- Fig. 16. Modelling of aeromagnetic and gravity data along line A-A', alternative (b) basement high, uppermost 10 km.
- Fig. 17. Modelling of aeromagnetic and gravity data along line A-A', alternative (c) thick sequence of volcanic rocks.

Fig. 18. Modelling of aeromagnetic and gravity data along line A-A', alternative (c) thick sequence of volcanic rocks, uppermost 10 km.

Fig. 19. Modelling of aeromagnetic and gravity data along line B-B', alternative (a) Mafic intrusions in or near the basement.

Fig. 20. Modelling of aeromagnetic and gravity data along line B-B', alternative (a) Mafic intrusions in or near the basement, uppermost 12 km.

Fig. 21. Modelling of aeromagnetic and gravity data along line B-B', alternative (b) Mafic intrusions in the deeper crust.

Fig. 22. Modelling of aeromagnetic and gravity data along line B-B', alternative (b) Mafic intrusions in the deeper crust, uppermost 12 km.

Tables

Table 1. Offshore aeromagnetic surveys compiled for the present interpretation.

Table 2. On land aeromagnetic surveys compiled for the present interpretation.

Table 3. Gravity surveys on land compiled in the present study.

Table 4. Density of sedimentary sequences from density logs of wells in the Nordland area.

Table 5. Seismic velocities (*1000 m/s) in the Nordland area.

Table 6. Magnetic properties of igneous rocks from drilling in the Vøring area within the Deep Sea Drilling Project (DSDP) and Ocean Drilling Program (ODP).

Table 7. Profile segments in composite line A-A'.

Bathymetry - topography Lofoten area

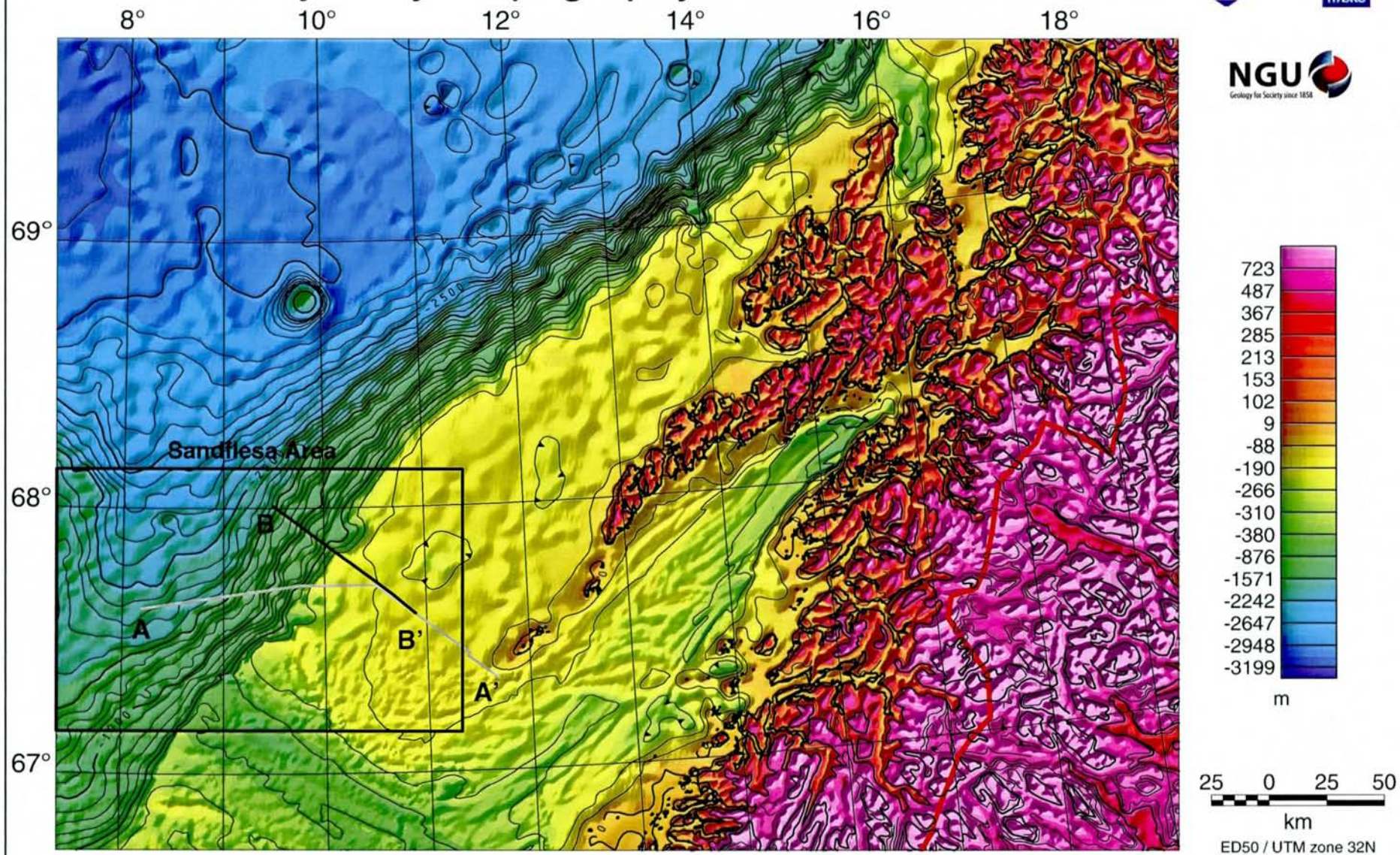


Fig. 1 Shaded relief, bathymetry and topography, 100 and 500 m contour intervals. Interpretation profile A-A' is shown on the map.

Basement faults - Lofoten area

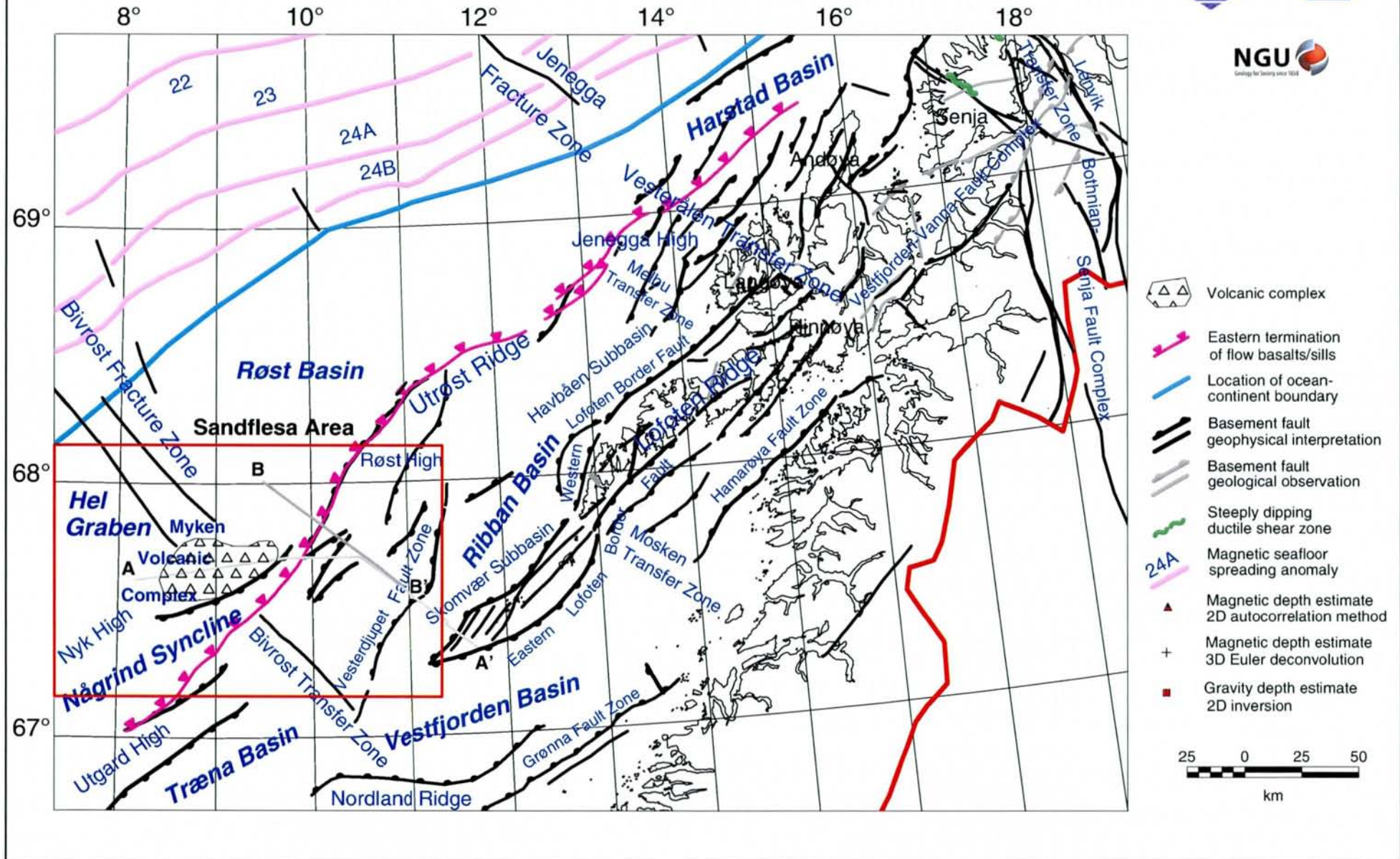


Fig. 2 Main structural elements within project area. Interpretation profiles A-A' and B-B' are shown on the map.

Aeromagnetic surveys - Lofoten area

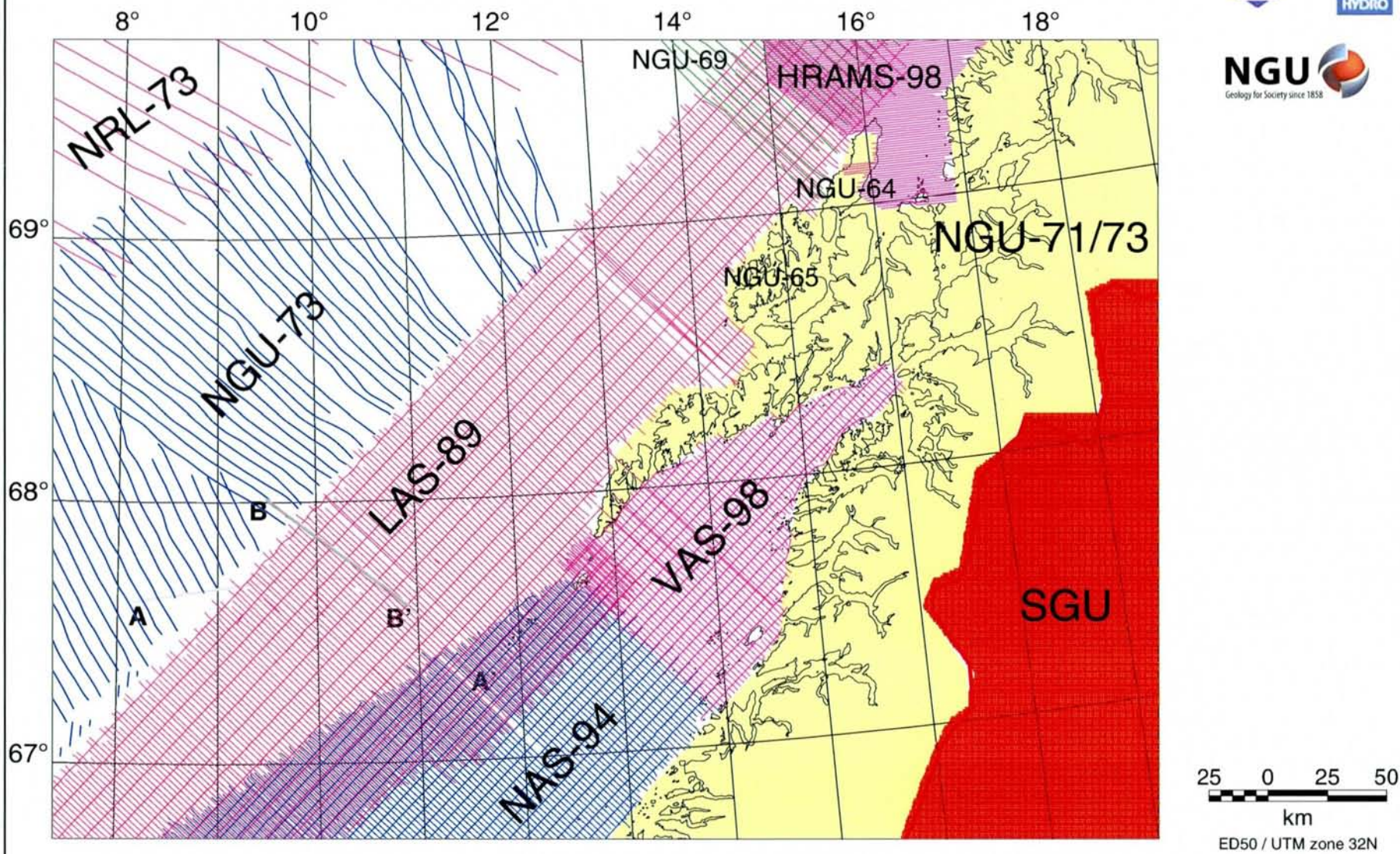


Fig. 3 Aeromagnetic database (Tables 1 & 2). Interpretation profiles A-A' and B-B' are shown on the map.

Gravity surveys - Lofoten area

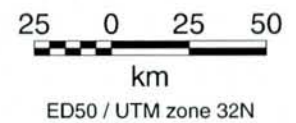
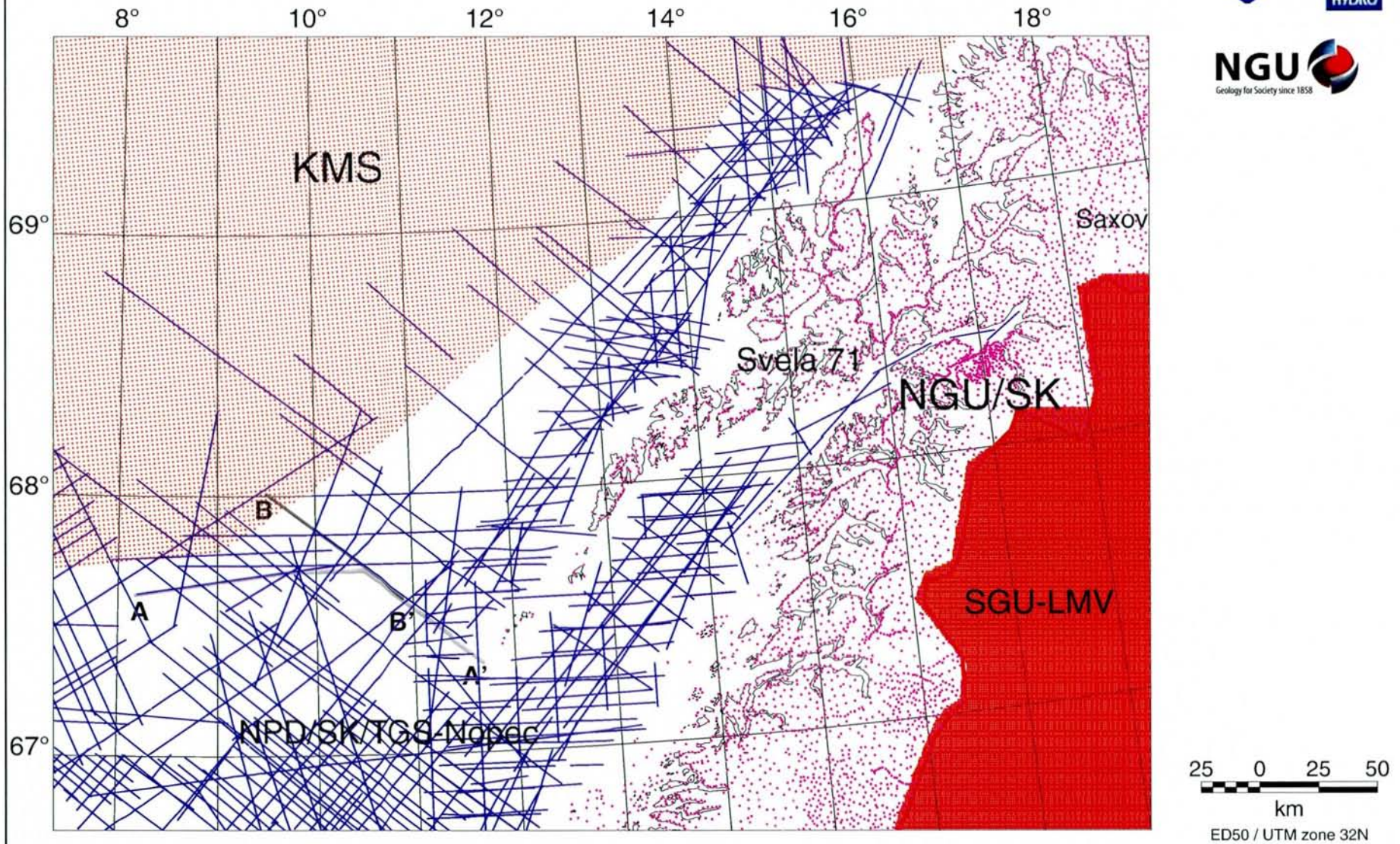


Fig. 4 Gravity database. Interpretation profiles A-A' and B-B' are shown on the map.

Magnetic total field referred to DGRF - Lofoten area

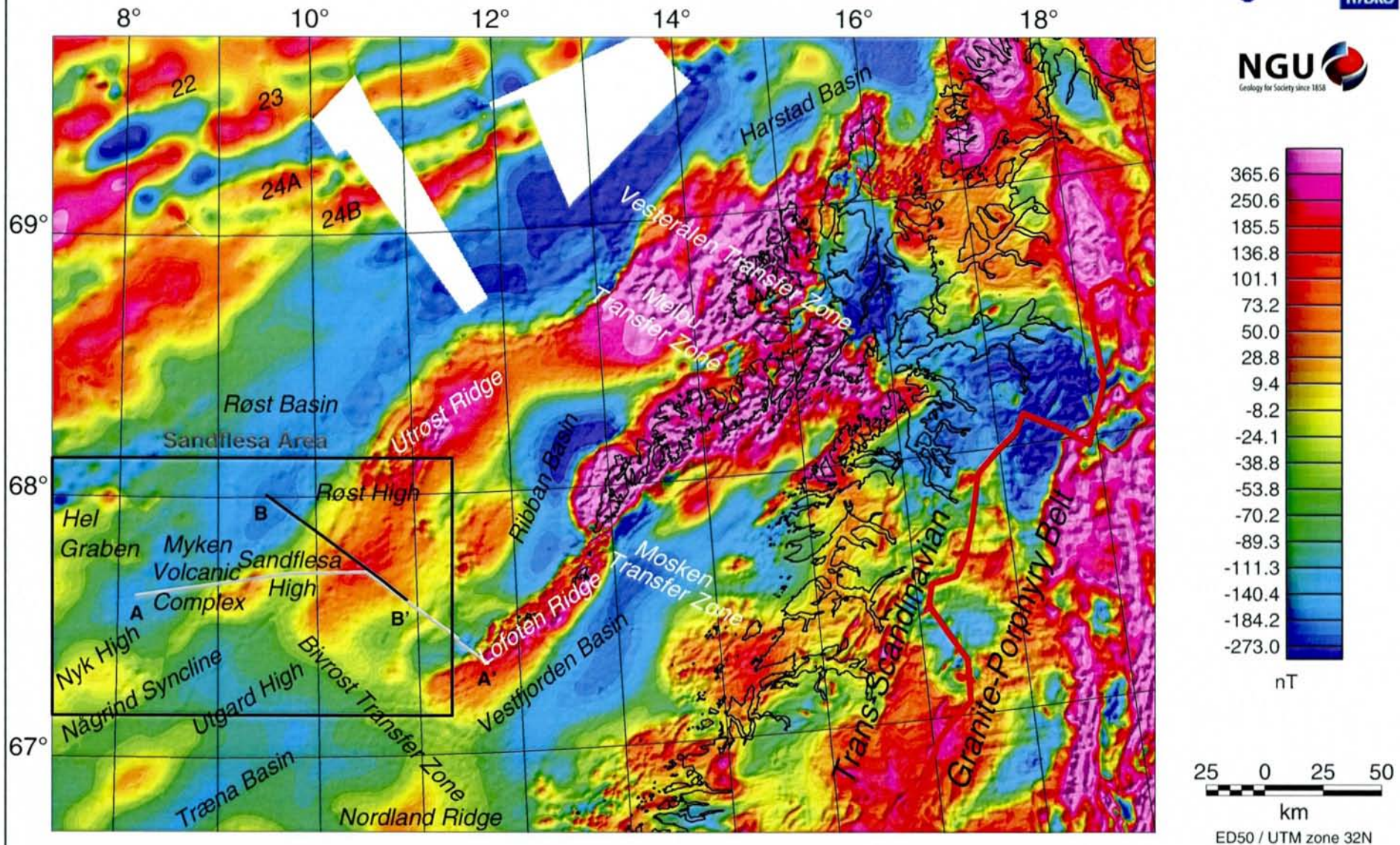


Fig. 5 Total magnetic field referred to DGRF. Interpretation profiles A-A' and B-B' are shown on the map.

Magnetic total field - 8 km highpass filtered - Lofoten area

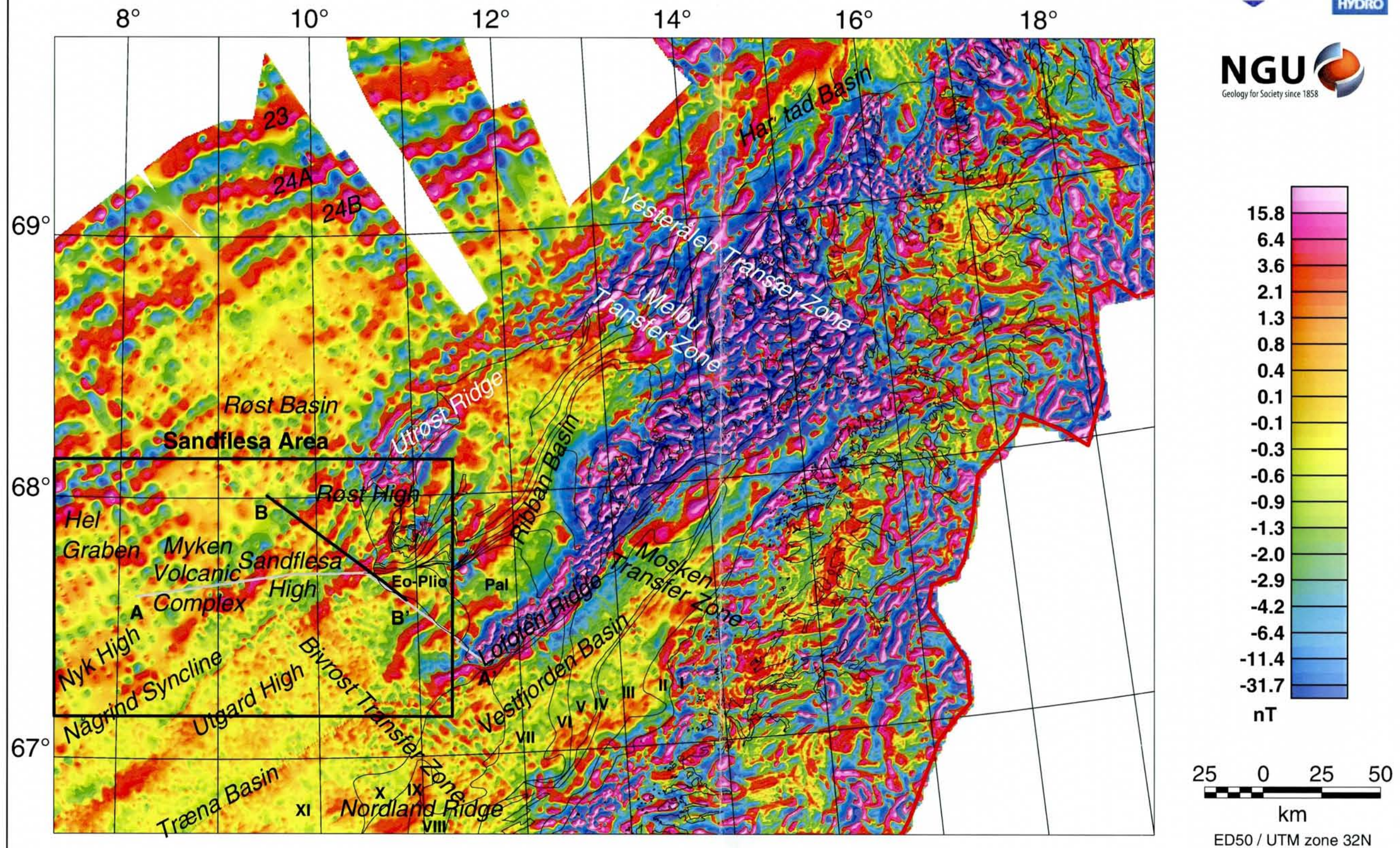


Fig. 6 Gaussian 8km high-pass filtered magnetic field. Subcrop interpretation and stratigraphy by Rokoengen et al. (1988) and Løseth & Fanavoll (1992) in the Vestfjorden Basin and the Ribban Basin, respectively, are added to the map.

Bouguer gravity - Isostatic residual - Lofoten area

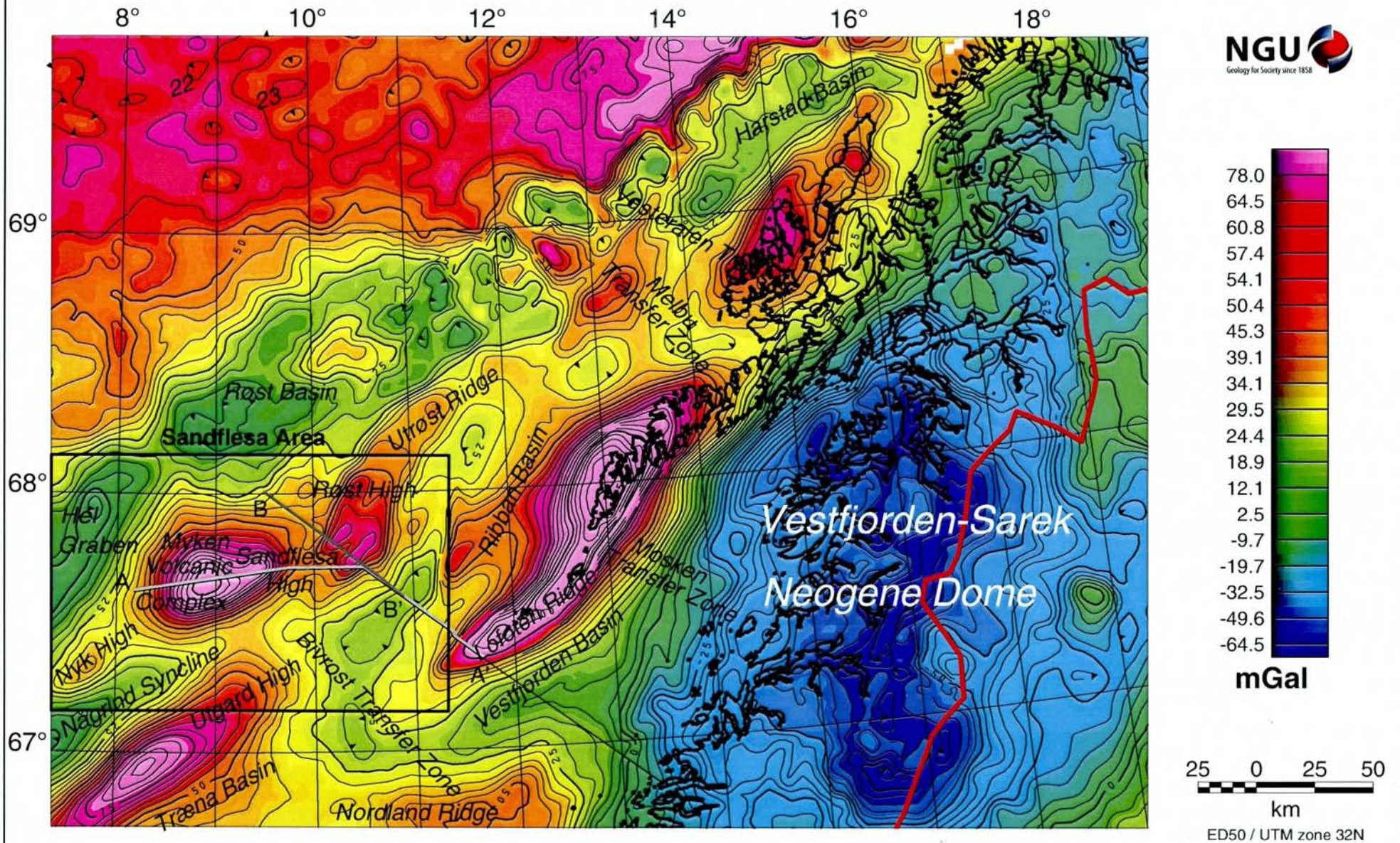


Fig. 7 Isostatic residual of Bouguer gravity.

Isostatic residual - Bouguer gravity - 100 km highpass filtered

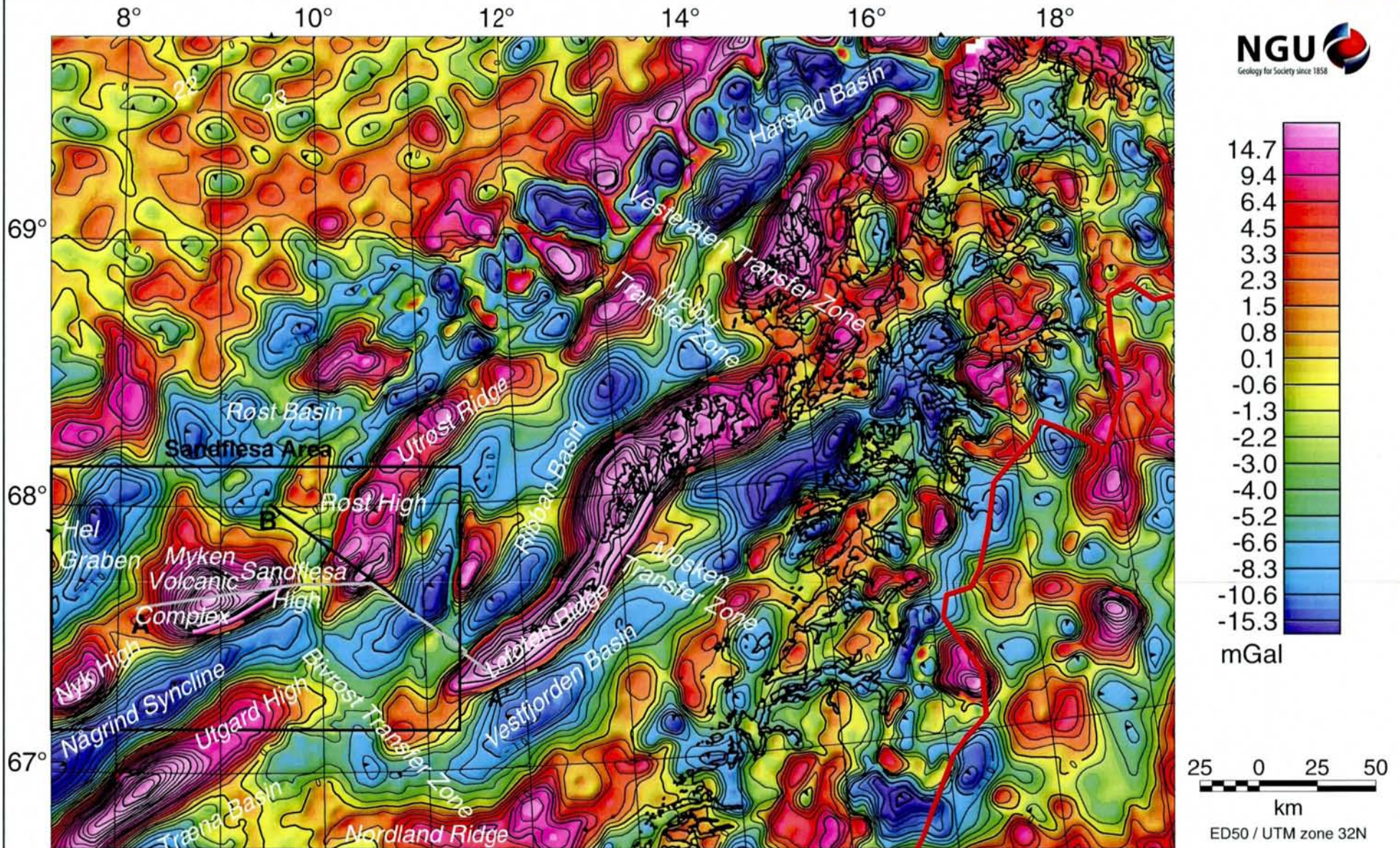


Fig. 8 Gaussian 100 km high-pass filtered isostatic residual, Bouguer gravity.

Basement structure map - Lofoten area

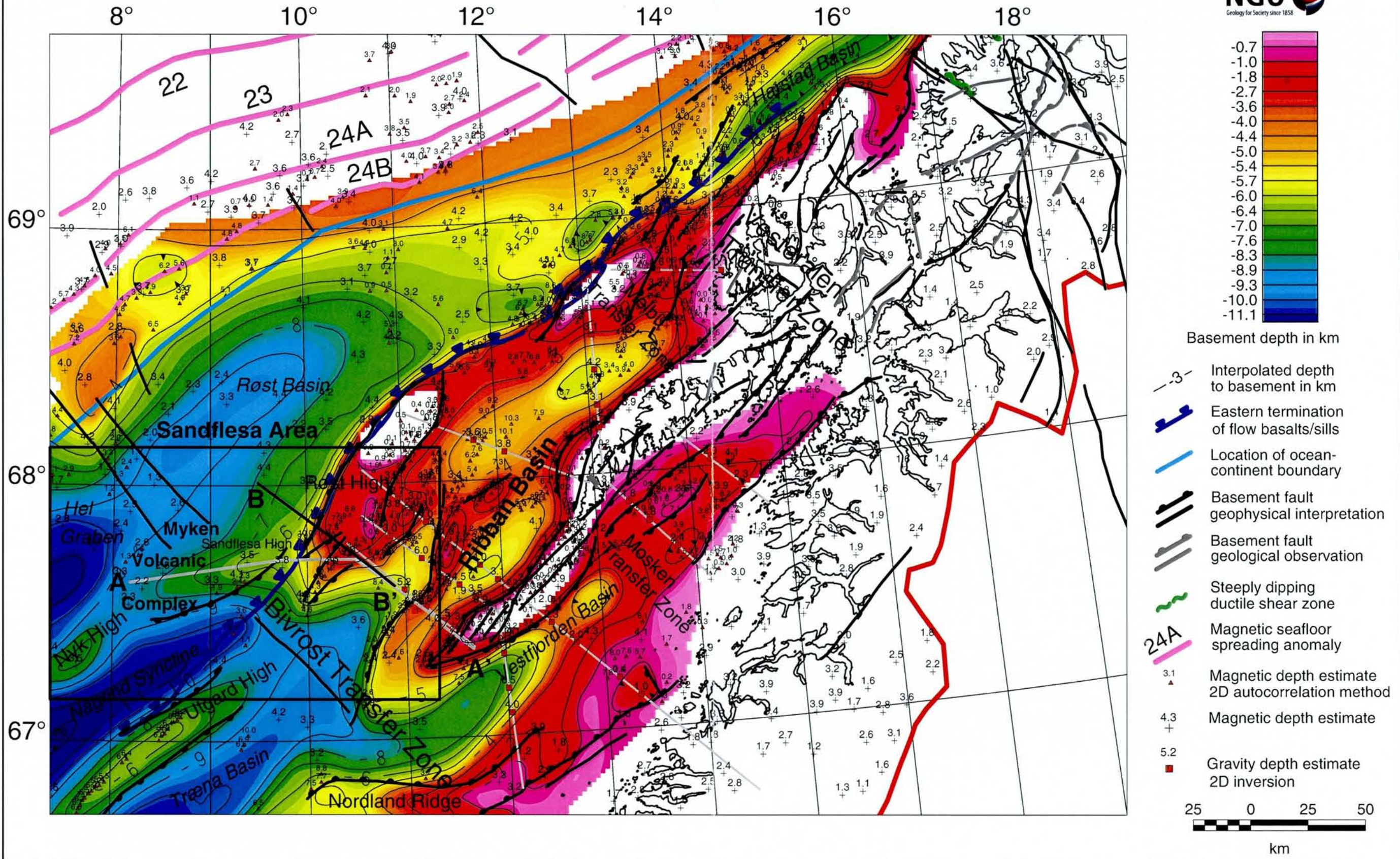


Fig. 9 Geophysical interpretation map Interpretation profiles A-A' and B-B' are shown on the map.

Aeromagnetic anomaly map - Sandflesa Area



Volcanic complex

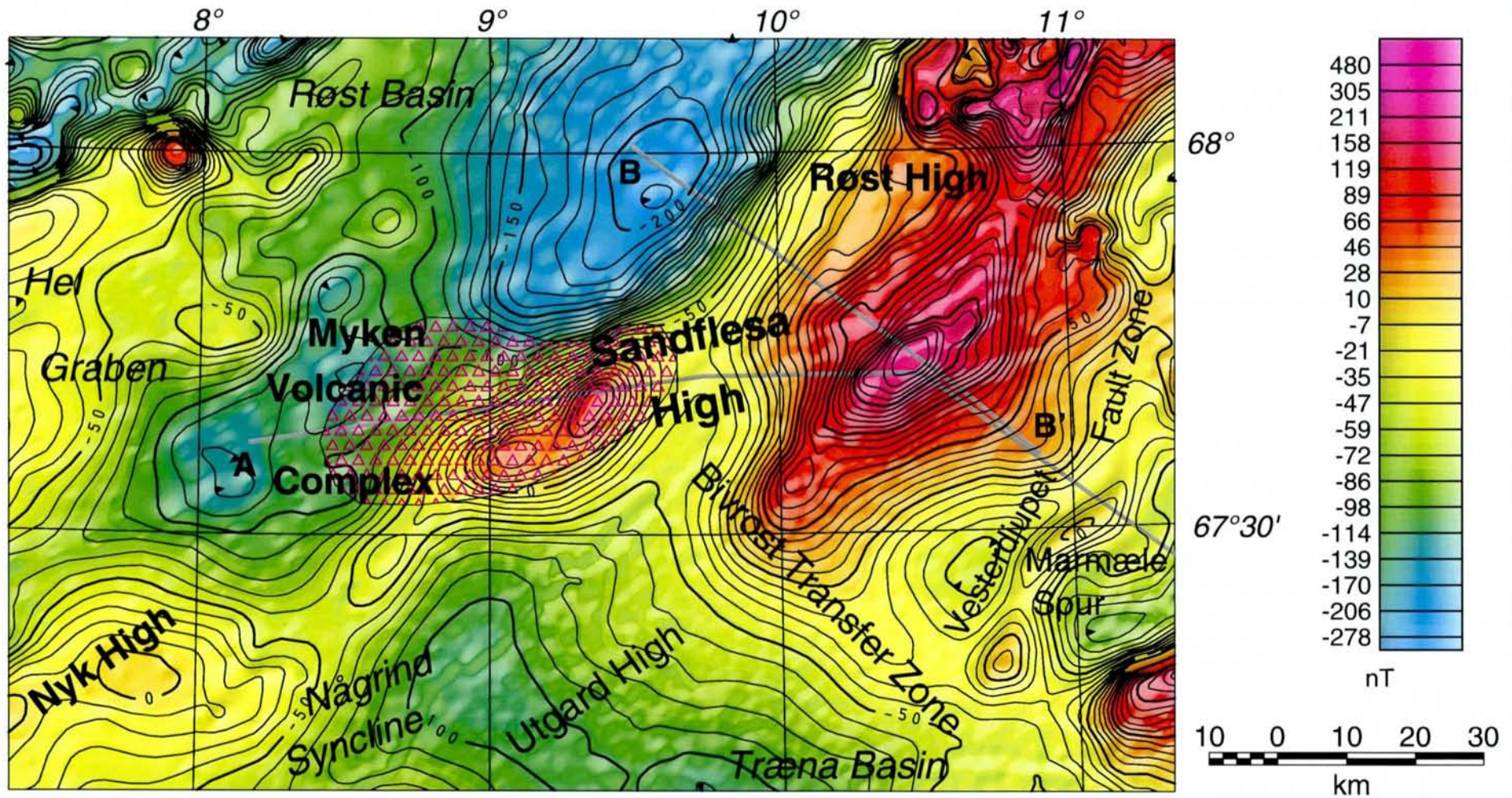


Fig. 10 Total magnetic field referred to DGRF. Sandflesa area. Interpretation profiles A-A' and B-B' are shown on the map.

Bouguer gravity, Isostatic residual - Sandflesa Area

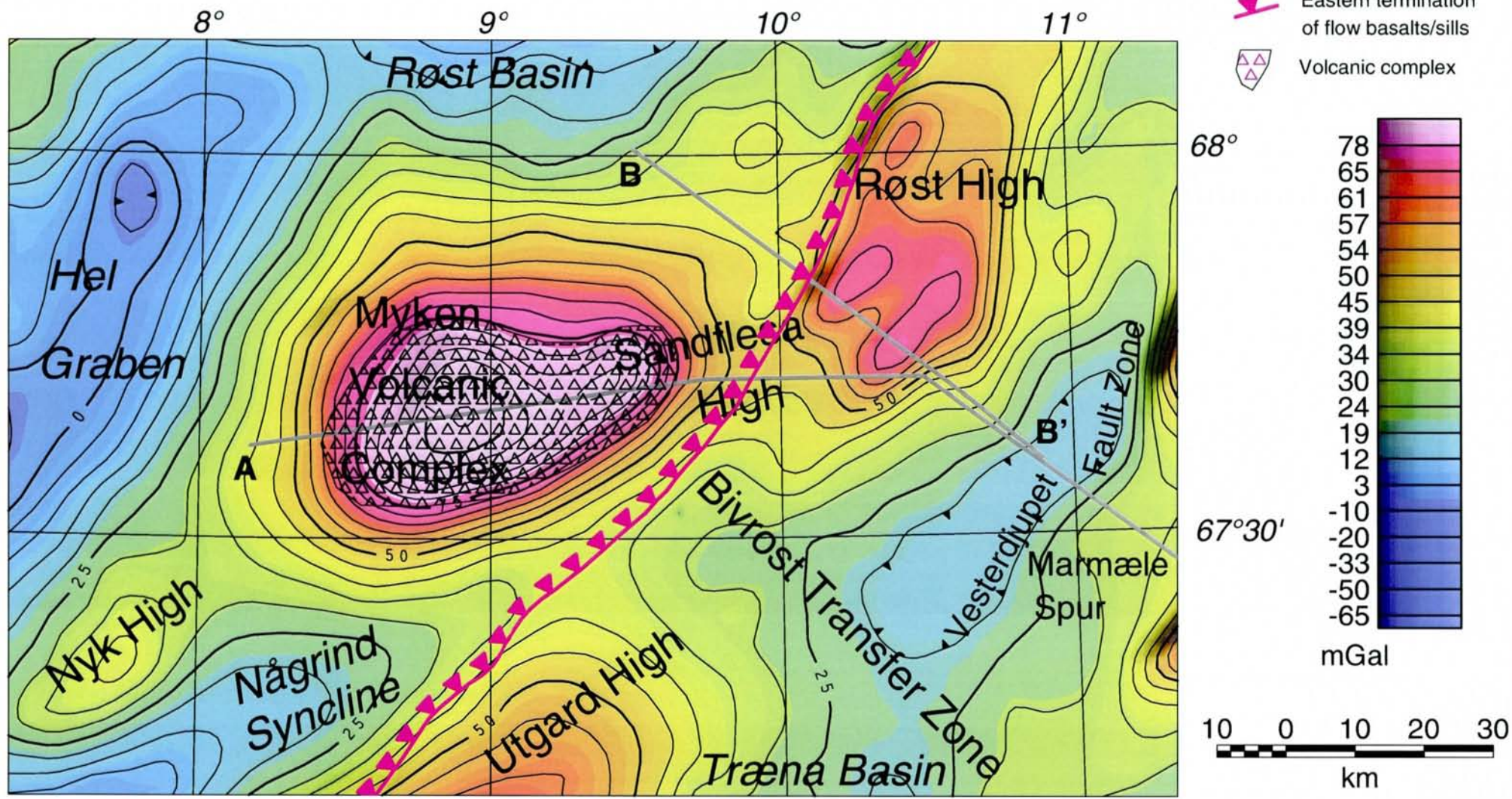


Fig. 11 Isostatic residual of Bouguer gravity, Sandflesa area.

Basement map - Sandflesa Area

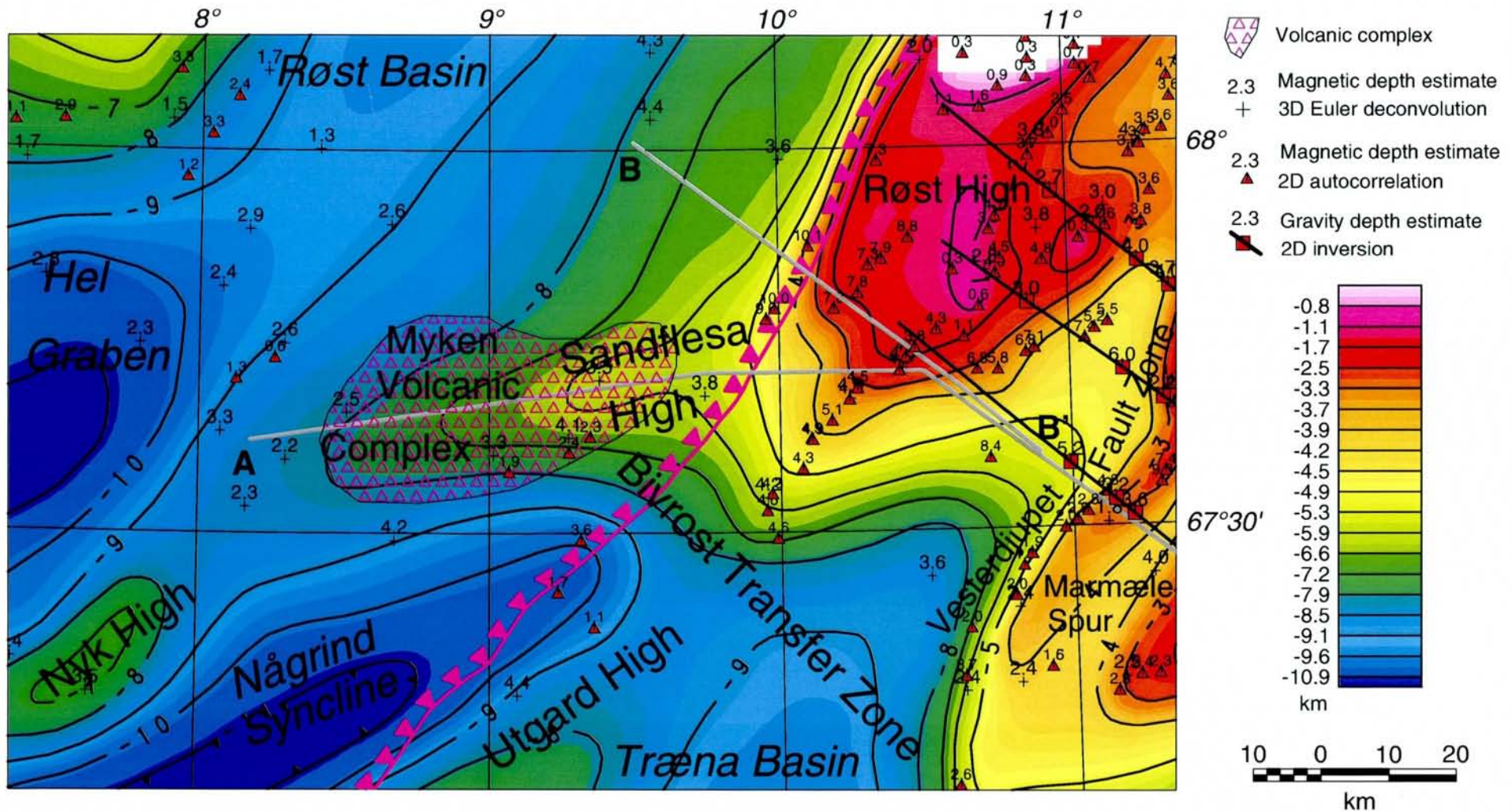


Fig. 12 Geophysical interpretation map. Sandflesa area. Interpretation profiles A-A' and B-B' are shown on the map.

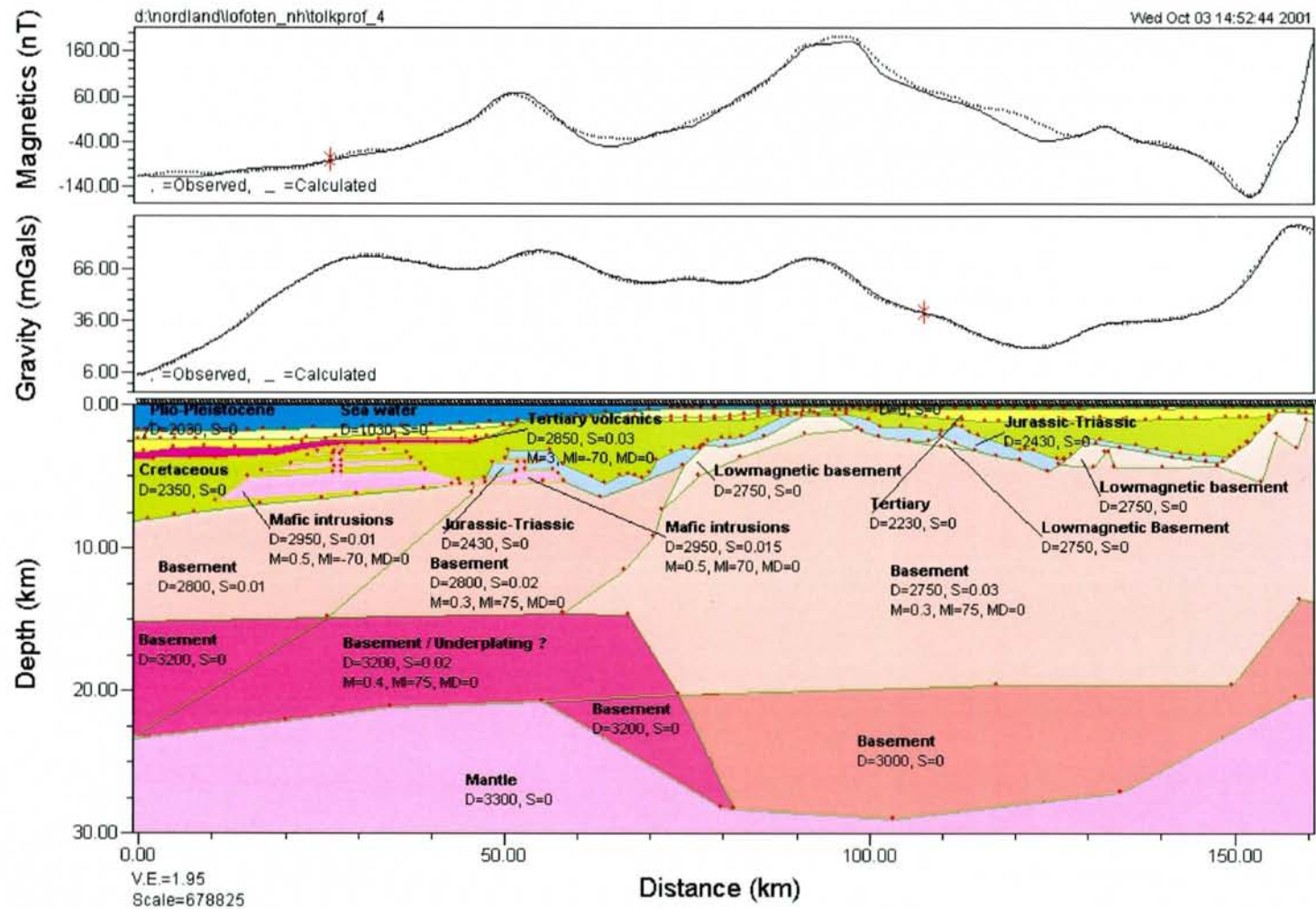


Fig. 13 Modelling of aeromagnetic and gravity data along line A-A', alternative (a) mafic volcanic intrusions.

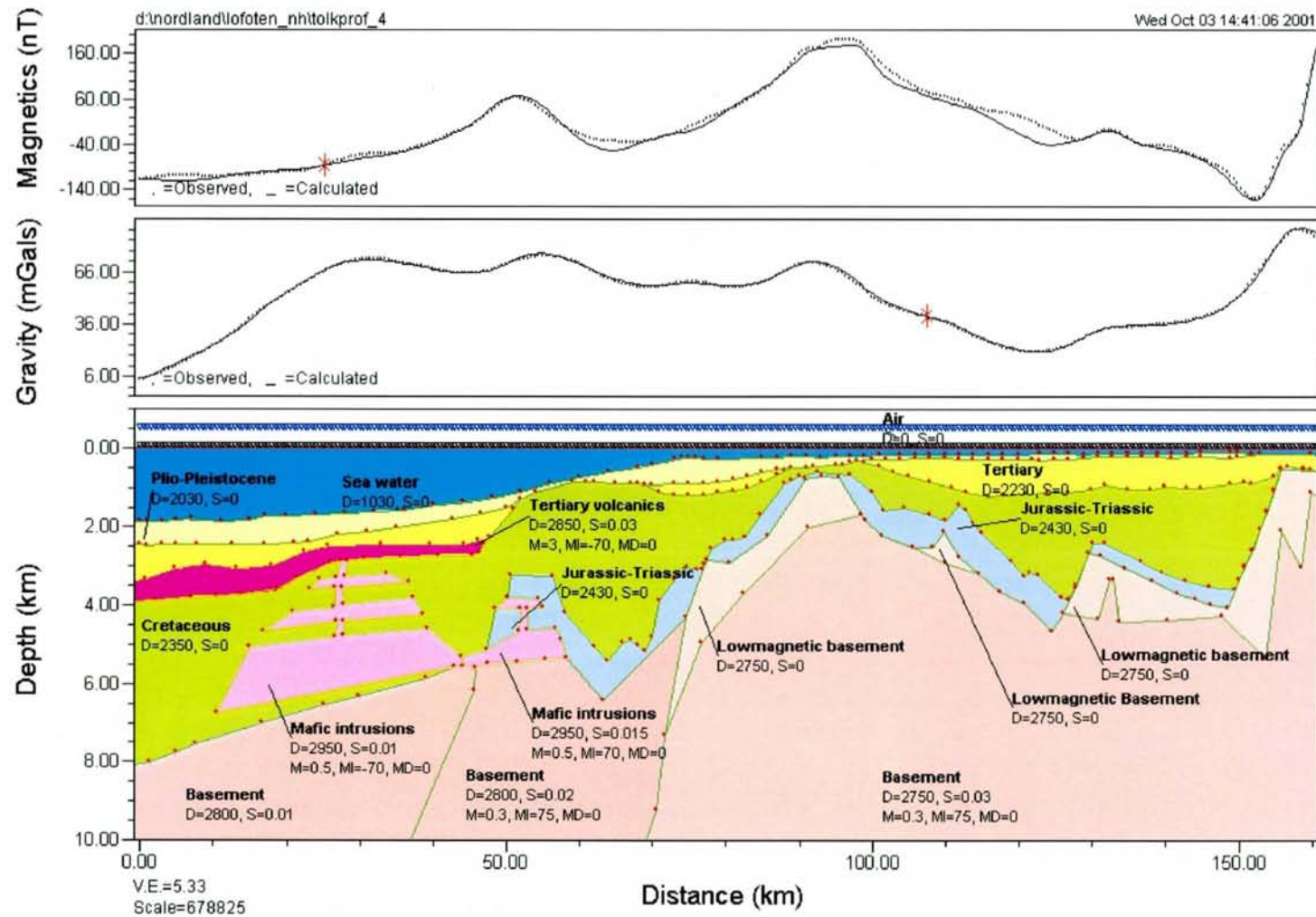


Fig. 14 Modelling of aeromagnetic and gravity data along line A-A', alternative (a) mafic volcanic intrusions, uppermost 10 km.

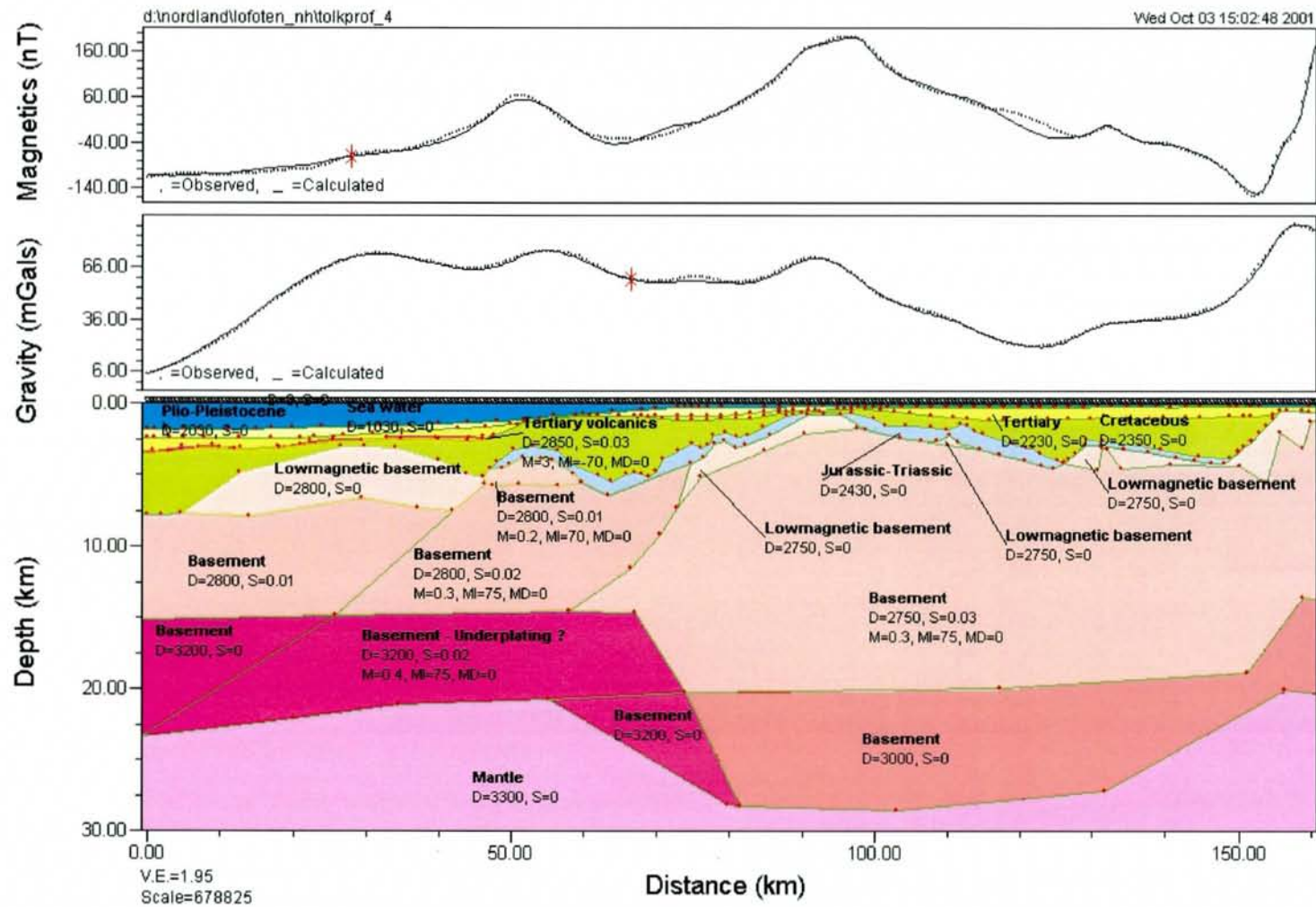


Fig. 15 Modelling of aeromagnetic and gravity data along line A-A', alternative (b) basement high.

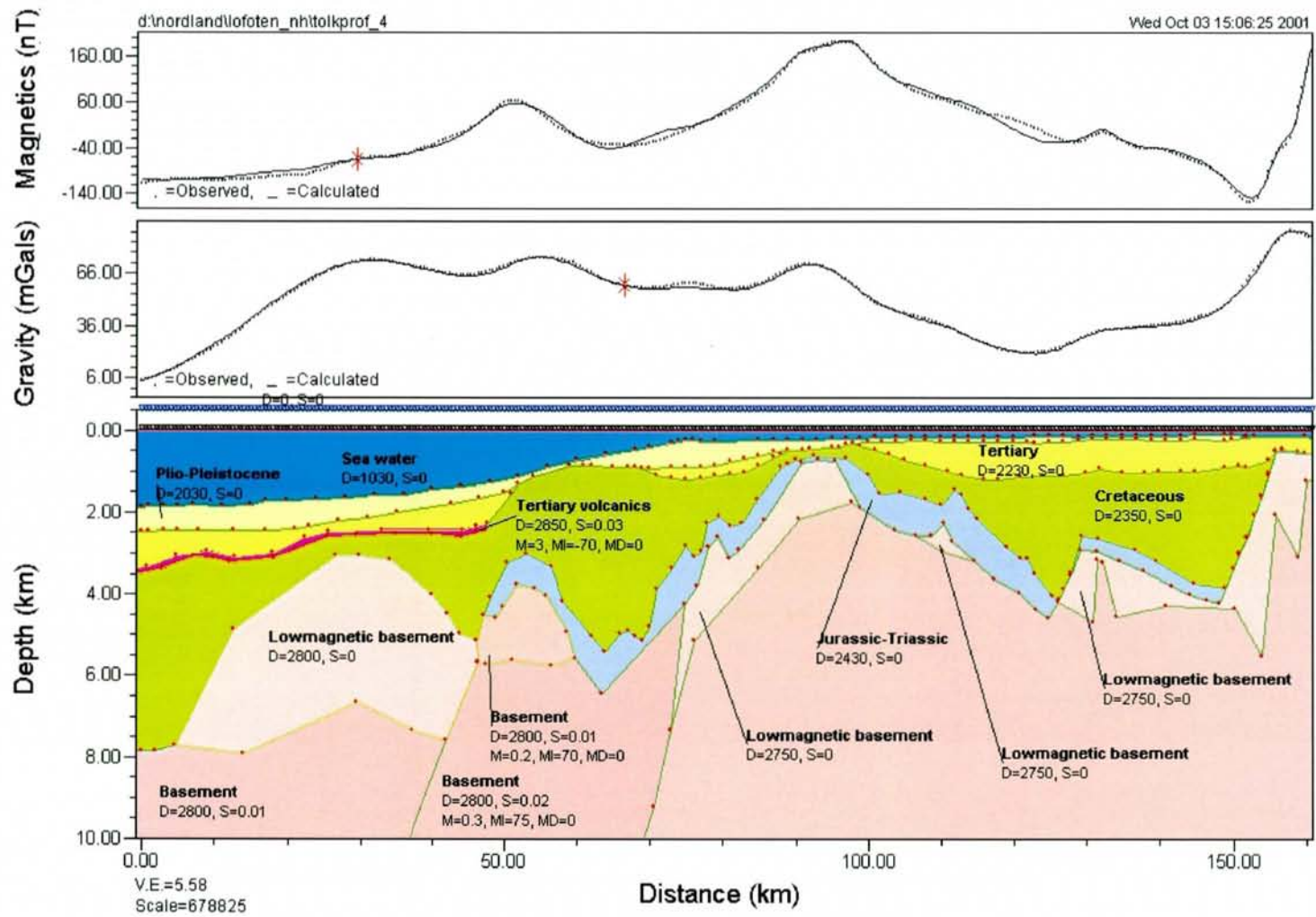


Fig. 16 Modelling of aeromagnetic and gravity data along line A-A', alternative (b) basement high, uppermost 10 km.

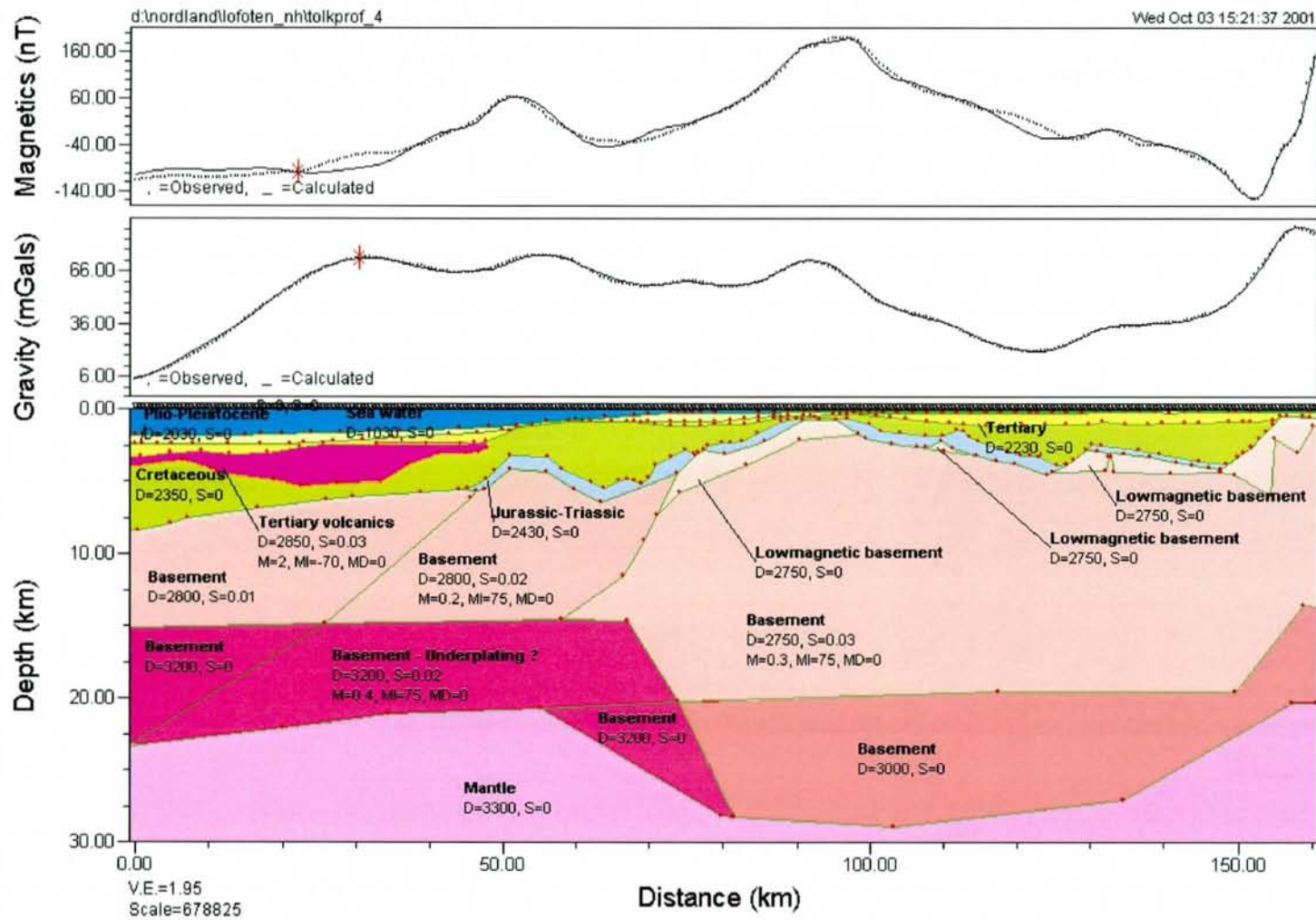


Fig. 17 Modelling of aeromagnetic and gravity data along line A-A', alternative (c) thick sequence of volcanic rocks.

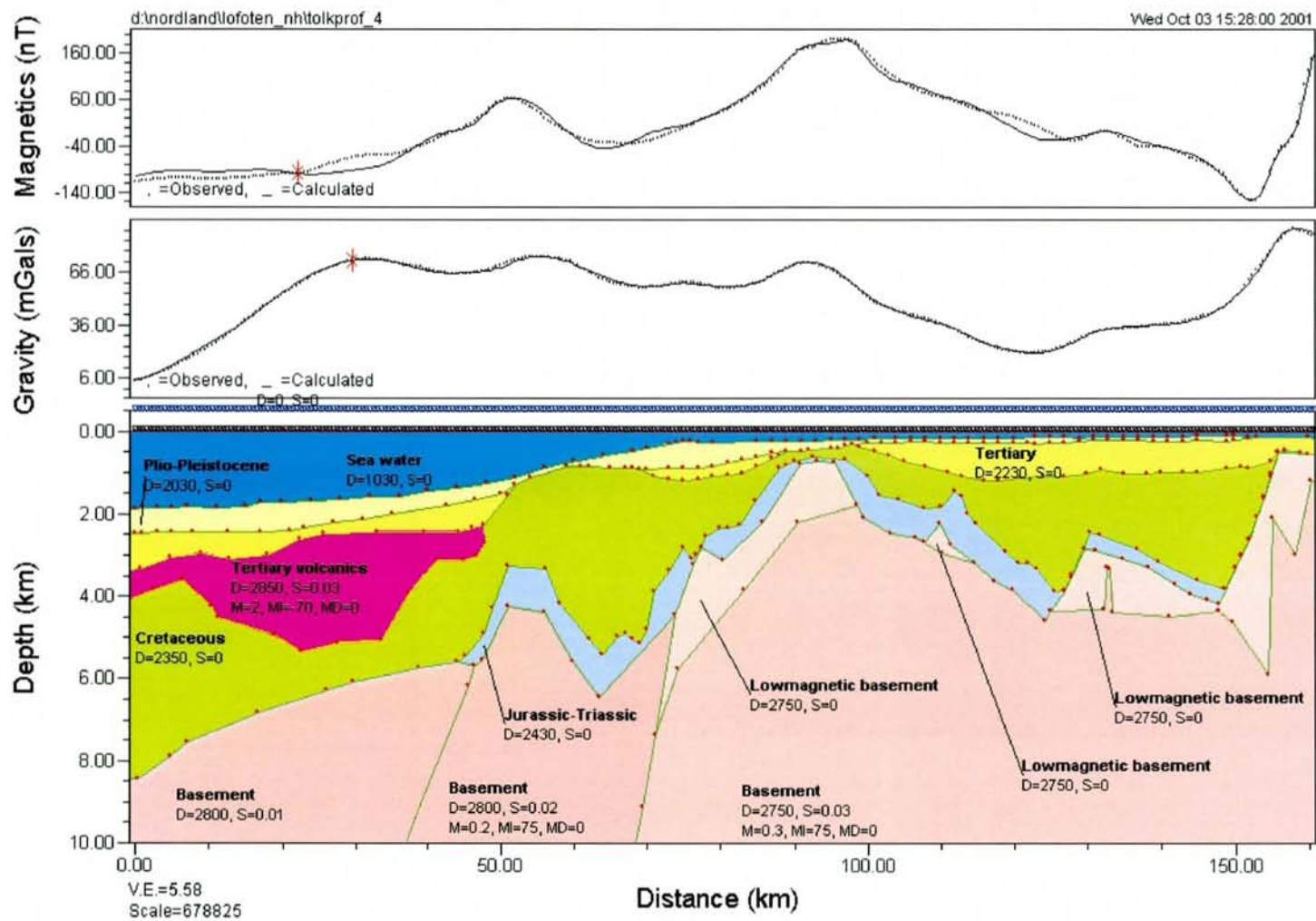


Fig. 18 Modelling of aeromagnetic and gravity data along line A-A', alternative (c) thick sequence of volcanic rocks, uppermost 10 km.

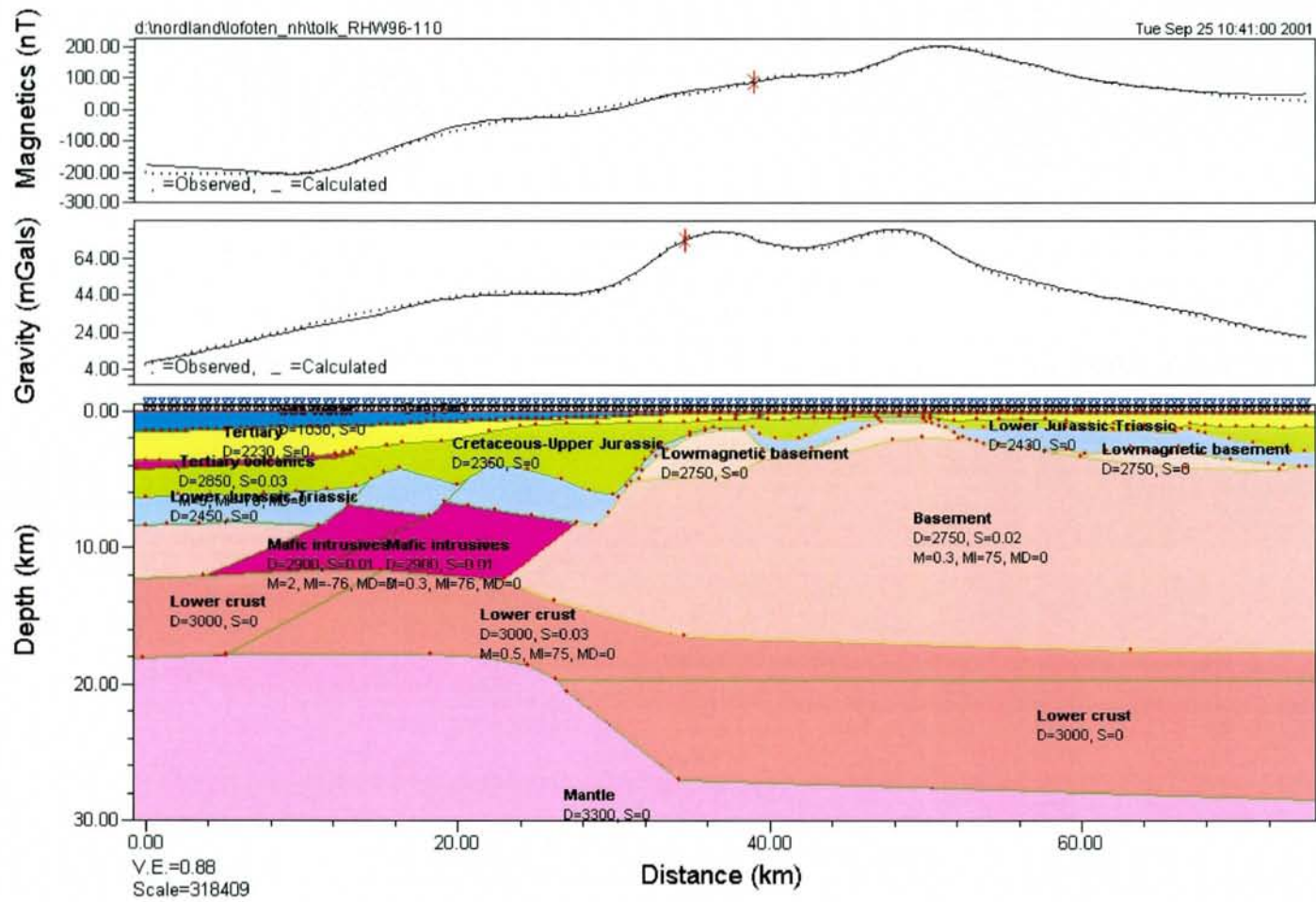


Fig. 19 Modelling of aeromagnetic and gravity data along line B-B', alternative (a) Mafic intrusions in or near the basement.

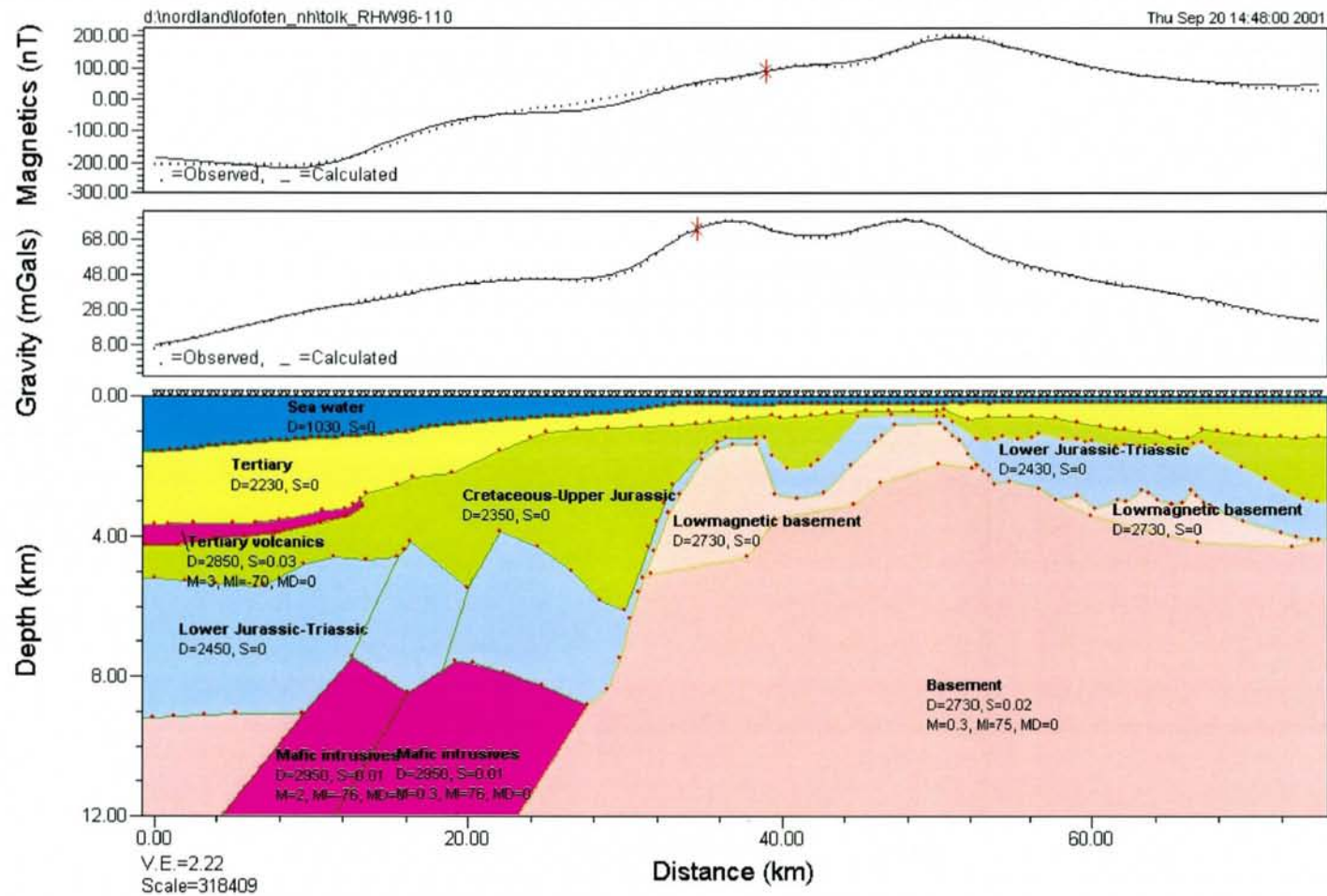


Fig. 20 Modelling of aeromagnetic and gravity data along line B-B', alternative (a) Mafic intrusions in or near the basement, uppermost 12 km.

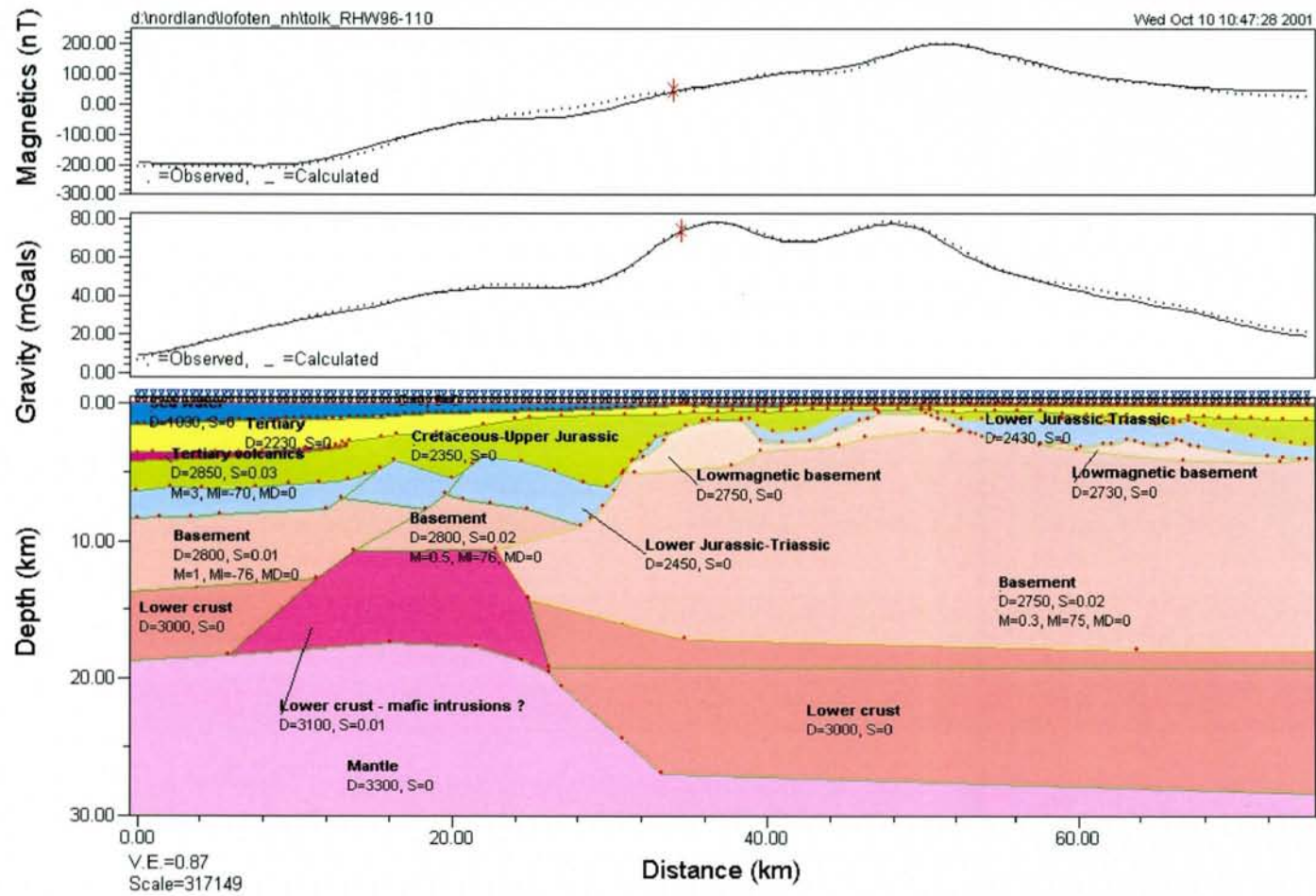


Fig. 21 Modelling of aeromagnetic and gravity data along line B-B', alternative (b) Mafic intrusions in the deeper crust.

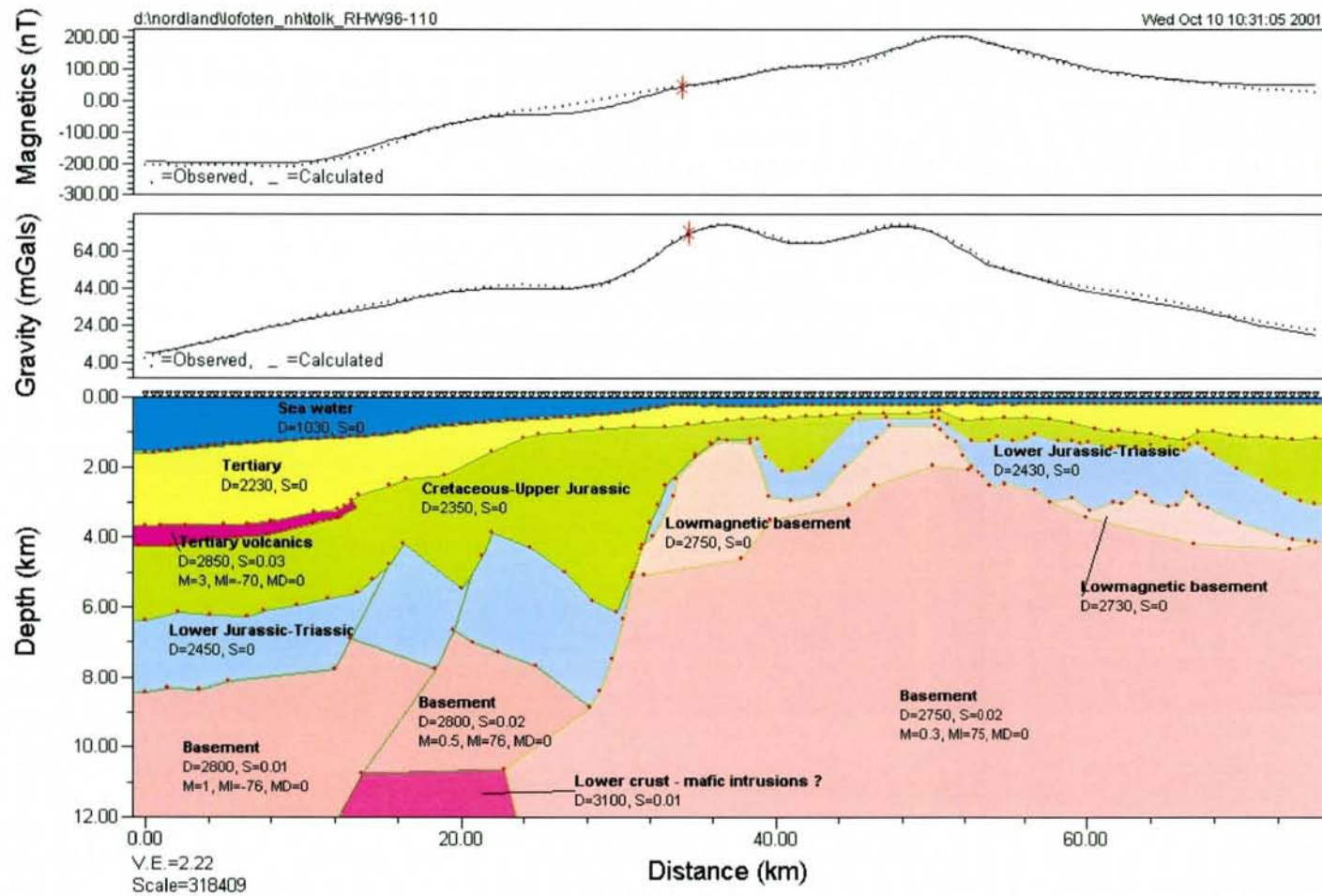


Fig. 22 Modelling of aeromagnetic and gravity data along line B-B', alternative (b) Mafic intrusions in the deeper crust, uppermost 12 km.